

## 1. Materials and methods

### 1.1. Animal model

Pregnant Sprague–Dawley rats were purchased from Shimizu laboratory (Kyoto, Japan). The day in which the vaginal plug was confirmed was considered to be day 0 of gestation (E0). In order to produce the fetal CDH rat model, 100 mg of nitrofen (2,4-dichlorophenyl-p-nitrophenylether: WAKO Chemical, Osaka, Japan) dissolved in 1 ml of olive oil was administered via an orogastric tube under short anesthesia on E9.5 (term, 22 days). As a control, some rats were given the same dose of olive oil without nitrofen. The animals were divided into three groups on E14: 1) CDH/BBS(+) group, in which the nitrofen-treated rats were administered BBS (50 µg/kg/day: Peptide Institute, Inc., Osaka, Japan) using an osmotic minipump (Alzet 2002: Palo Alto, CA, USA) implanted in the peritoneal cavity under general anesthesia; 2) CDH/BBS(−) group, in which the nitrofen-treated rats were administered normal saline instead of BBS using an osmotic minipump; and 3) control group, in which rats treated without nitrofen were administered normal saline instead of BBS using an osmotic minipump. The fetuses were harvested via cesarean section and weighed on E21. The peritoneal cavity of each fetus was opened and a defect in the diaphragm was confirmed with a visual inspection of the diaphragm. The bilateral lungs were removed and weighed, and the lung-body-weight ratio (both lungs (mg)/body (g) weight: LBWR) was measured. The expression of proliferating cell nuclear antigen (PCNA) was assessed using both immunohistochemical staining and real-time polymerase chain reaction (PCR) in order to determine the amount of cell proliferation. The degree of lung maturity was assessed as the expression of thyroid transcription factor-1 (TTF-1), a marker of alveolar epithelial cell type II.

### 1.2. Immunohistochemical staining

The left lungs were immersed and fixed in 4% paraformaldehyde for eight hours and embedded in paraffin. The samples were cut into 5-µm-thick sections and deparaffinized. Subsequently, antigen retrieval was performed by boiling the sections in a 10 mmol/L of sodium citrate solution at a pH of 6.0 for two periods of five minutes in a microwave at medium heat. After rinsing the slides in PBS, the endogenous peroxidase activity was blocked by exposing the slides to a 3% hydrogen peroxide in methanol solution for a period of 10 minutes.

To detect positive cells of PCNA or TTF-1 in the lungs, immunohistochemical staining was performed using a primary antibody to rat PCNA (PC10: Nichirei, Tokyo, Japan) or TTF-1 (SPT24: Nichirei, Tokyo, Japan). The sections were incubated with the primary antibodies for one hour at room temperature. The primary antibodies were visualized using the Histofine Simple Stain MAX-PO (M) kit (Nichirei, Tokyo, Japan) according to the instruction manual. The slide was counterstained with hematoxylin. Using a Dynamic Cell Count (BZ-H1C: Keyence, Tokyo, Japan) with high power field (×400), the number of positive cells was counted and averaged for five sites in each group.

### 1.3. RT-PCR and real-time RT-PCR

The left lungs obtained from the three groups, control (n = 8), CDH/BBS(−) (n = 7) and CDH/BBS(+) (n = 7), were analyzed. Total RNA was extracted according to the guanidinium acid phenol method using ISOGEN II (Nippon gene, Toyama, Japan). In addition, total RNA was reverse transcribed using ReverTra Ace® qPCR RT Master Mix (Toyobo, Tokyo, Japan) according to the manufacturer's instructions.

Real-time reverse transcription-PCR (RT-PCR) was performed using the Real-time PCR Master Mix (Toyobo, Tokyo, Japan) and the 7500 Real-Time PCR Systems (Applied Biosystems, Foster, CA, USA) according to the manufacturer's instructions. The matching primers for PCNA (Rn01514538\_g1), TTF-1 (Rn01436110\_m1) and β-actin (Rn014244440\_s1) were purchased from Applied Biosystems.

### 1.4. Statistical analysis

The statistical analysis was performed using Student's *t*-test for unequal variances. A *p* value of less than 0.05 was considered to be statistically significant.

## 2. Results

The incidence of CDH in this study was 50% (13/26 fetuses) among the nitrofen-treated rats not administered BBS and 49% (24/49) in those administered BBS. The defect in the diaphragm was observed on the left side in all CDH fetuses, and no other anomalies were found.

There were no significant differences in body weight between the CDH/BBS(−) group and the CDH/BBS(+) group. The LBWR values were compared between the three groups: control (nitrofen(−), BBS(−)) (n = 23), CDH/BBS(−) (nitrofen(+), BBS(−)) (n = 13), and CDH/BBS(+) (nitrofen(+), BBS(+)) (n = 24). Consequently, the LBWR in the CDH/BBS(−) group was significantly less than that observed in the control group (16.05 ± 2.32 v.s. 23.86 ± 2.78; *p* < 0.01). On the other hand, the LBWR in the CDH/BBS(+) group was significantly greater than that observed in the CDH/BBS(−) group (18.29 ± 3.03 v.s. 16.05 ± 2.32; *p* < 0.05) (Fig. 1).

Regarding the immunohistochemical stainings, both PCNA- and TTF-1-positive cells were localized to the alveolar endothelium in the fetal rats. The number of PCNA-positive cells in the CDH/BBS(−) group was significantly greater than that observed in the control group (877.0 ± 87.8 v.s. 290.4 ± 50.65; *p* < 0.01). Meanwhile, the number of PCNA-positive cells in the CDH/BBS(+) group was less than that observed in the CDH/BBS(−) group (501.8 ± 72.7 v.s. 877.0 ± 87.8; *p* < 0.01) (Fig. 2). In addition, the number of TTF-1-positive cells in the CDH/BBS(−) group was significantly greater than that observed in the control group (664.0 ± 90.5 v.s. 238.4 ± 52.8; *p* < 0.01). Conversely, the number of TTF-1-positive cells in the CDH/BBS(+) group was significantly less than that observed in the CDH/BBS(−) group (267.6 ± 30.0 v.s. 664.0 ± 90.5; *p* < 0.01) (Fig. 3).

On RT-PCR, the mRNA expression levels of PCNA (PCNA/β-actin) were low in the CDH/BBS(+) group. However, there were no significant differences between the CDH/BBS(−) and CDH/BBS(+) groups (2.49 ± 1.11 v.s. 1.69 ± 0.58) (Fig. 4). On the other hand, the mRNA expression levels of TTF-1 (TTF-1/β-actin) in the CDH/BBS(+) group were significantly decreased compared with those observed in the CDH/BBS(−) group (2.55 ± 1.21 v.s. 1.45 ± 0.23; *p* < 0.05) (Fig. 5).

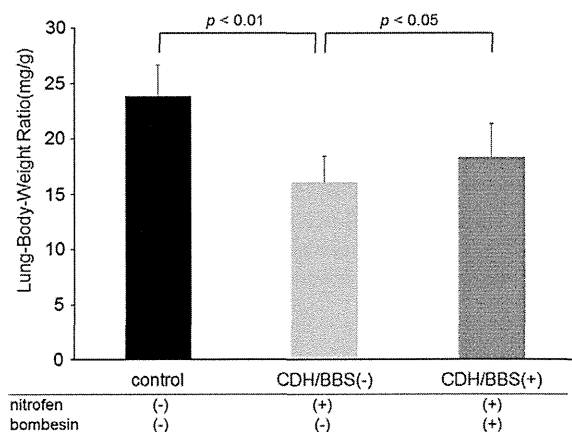
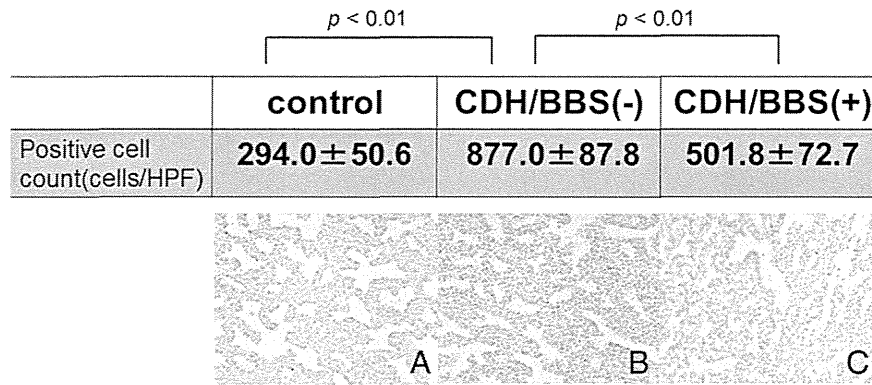


**Fig. 1.** Lung-body-weight ratio (LBWR) values in the control, CDH/BBS(−) and CDH/BBS(+) groups. The LBWR values in the control group were significantly greater than those observed in the CDH/BBS(−) group (*p* < 0.01). The LBWR values in the CDH/BBS(+) group were also significantly greater than those observed in the CDH/BBS(−) group (*p* < 0.05).



BBS: bombesin, CDH: congenital diaphragmatic hernia  
HPF : high power field

**Fig. 2.** Immunohistochemical staining for PCNA. Micrographs show the nuclear localization of PCNA and TTF-1 in the lung alveolar epithelium. The number of PCNA-positive cells in the CDH/BBS(–) group was significantly greater than that observed in the control group. Meanwhile, the number of PCNA-positive cells in the CDH/BBS(+) group was less than that observed in the CDH/BBS(–) group. PCNA staining; control group (A), CDH/BBS(–) group (B), CDH/BBS(+) group (C) Original magnification: ×400.

**3. Discussion**

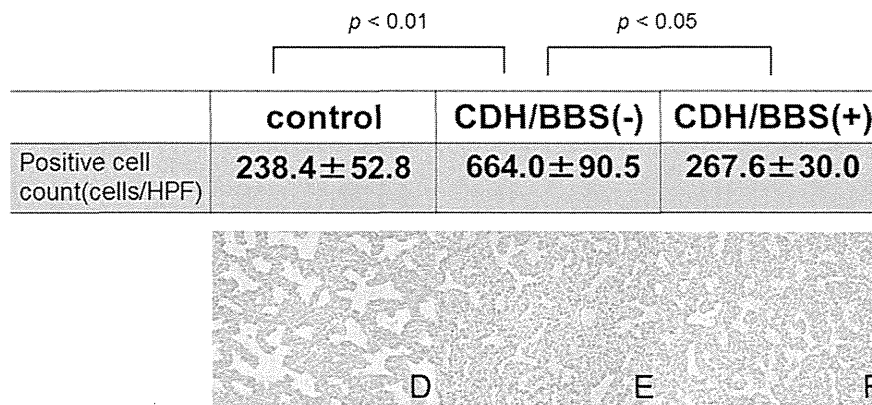
The present study demonstrated that the prenatal administration of BBS promotes lung growth and maturity in a rat model of nitrofen-induced CDH without inducing other serious anomalies. To our knowledge, there have been no previous reports showing that prenatal medical treatment increases fetal lung weight in a rat nitrofen-induced CDH model.

The use of prenatal medical treatment with corticosteroids in fetuses with CDH has been reported both experimentally and clinically [17]. There are many reports showing that the antenatal administration of corticosteroids may correct lung immaturity; however, no experiments using corticosteroids have succeeded in increasing the fetal lung volume. With respect to clinical studies, late gestational maternal corticosteroid administration has been found to have no effect in improving fetal lung hypoplasia to date [18].

There are various experimental reports indicating that the administration of antenatal retinoic acid affects the expression of various genes related to lung maturity in CDH rat models [19–21], and Montedonico et al. found that prenatal treatment with retinoic acid stimulates alveologenesis in hypoplastic lungs under the setting of CDH [22]. However, Gonzalez-Reyes et al. reported no changes in the lung weight-to-body

weight ratio using similar rat models [23]. Furthermore, retinoic acid appears to be unlikely as a candidate of prenatal treatment for CDH, because the prenatal administration of this agent carries the potential risk of inducing many major anomalies, such as intestinal atresia and anorectal malformations [24]. As a pilot study, we investigated the effect of BBS to pregnant rats without nitrofen administration from day 1 to investigate whether BBS might have other effect to the fetus. As a result, it was confirmed that there were no increase of lung volume and no major anomalies found in fetuses. In the present study, no other anomalies were found in the nitrofen-induced rat CDH model and the additional administration of BBS did not induce any further anomalies. Considering the potential for teratogenic risk and safety, BBS may be a candidate for use in prenatal medical therapy. In order to access the actual effect of BBS to lung of CDH rat in this study, the parameters of lung maturation were compared between CDH/BBS(–) group and CDH/BBS(+) group.

In this study, both PCNA and TTF-1 were used as markers of lung maturation. The number of PCNA-positive cells is increased in immature lungs. Similarly, in our CDH model with lung hypoplasia, both the number of PCNA-positive cells and the mRNA expression of it were significantly increased, thus indicating that lungs in our CDH model were immature ones. TTF-1 is a marker of alveolar epithelial cells type II



BBS: bombesin, CDH: congenital diaphragmatic hernia  
HPF : high power field

**Fig. 3.** Immunohistochemical staining for TTF-1. Micrographs show the nuclear localization of TTF-1 in the lung alveolar epithelium. The number of TTF-1 positive cells in the CDH/BBS(–) group was significantly greater than that observed in the control group. The number of TTF-1 positive cells in the CDH/BBS(+) group was less than that observed in the CDH/BBS(–) group. TTF-1 staining; control group (D), CDH/BBS(+) group (E), CDH/BBS(+) group (F).

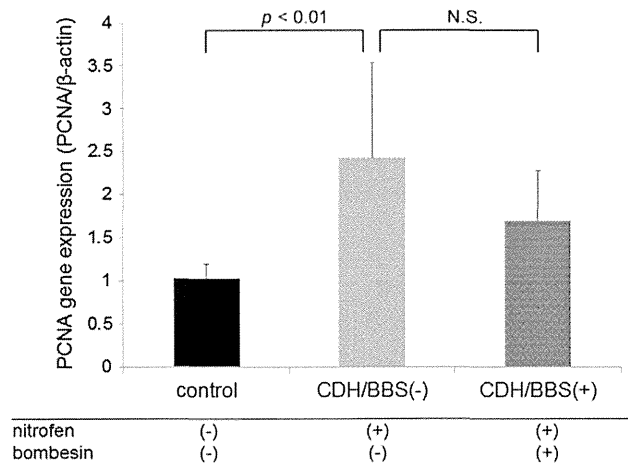


**Fig. 4.** mRNA expression levels of PCNA on RT-PCR. The expression levels of PCNA were increased in the lungs of the CDH/BBS(–) group compared to that observed in the control group ( $p < 0.01$ ). There were no significant differences between the CDH/BBS(–) and CDH/BBS(+) groups.

(AECs-II). It has been reported that the AEC-II levels are also increased in the hypoplastic lungs of animals with CDH [25]. In the present study, it was also confirmed that both the number of TTF-1-positive cells and the mRNA expression of TTF-1 in the CDH group were also significantly increased, compared with that observed in the control group. Therefore, based on our results in PCNA and TTF-1, the hypoplastic lungs in our rat CDH model indicated to be immature.

As for the effect of BBS administration on fetal lung maturity, the expression levels of PCNA and TTF-1 were significantly decreased in the CDH/BBS(+) group. Our results showed BBS was considered to have promoted fetal lung maturity. As described previously, we investigated the effects of the BBS and elucidated its multipotent ability to maintain and modulate the mucosal structure and immunity of the gastrointestinal system [6–10]. Based on present and previous data, we speculate that BBS plays an important role via the same pathways in the respiratory and intestinal mucosa systems. In this study, it is impossible to deny that BBS affected maternal metabolism and had some secondary effect to the fetus. However, in our previous study of rat intestinal transplantation, it was confirmed that BBS surely had direct effect on the intestinal mucosal system. Therefore, we now speculate that BBS affected directly the lung of the fetuses as well as their intestine.

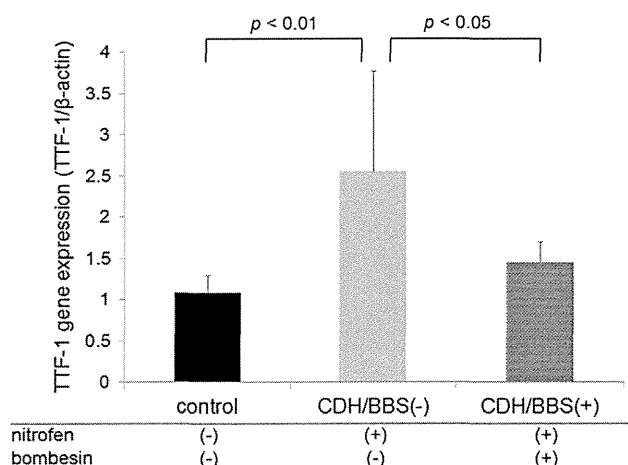


**Fig. 5.** mRNA expression levels of TTF-1 on RT-PCR. The expression levels of TTF-1 were increased in the lungs of the CDH/BBS(–) group compared to that observed in the control group ( $p < 0.01$ ) and CDH/BBS(+) group ( $p < 0.05$ ).

In conclusion, the prenatal administration of the neuropeptide bombesin increases the fetal lung volume and promotes fetal lung maturity without inducing other anomalies in a rat nitrofen-induced CDH model. The prenatal administration of neuropeptide BBS may be a possible candidate therapy for improving lung hypoplasia in patients with fetal CDH.

## Acknowledgments

This work was supported by Grant-in-Aid for Exploratory Research from the Ministry of Education, Culture, Sports, Science and Technology of Japan (MEXT KAKENHI grant number 22659318).

The English used in this manuscript was reviewed by Brian Quinn (Editor-in-Chief, Japan Medical Communication).

## References

- [1] Doyle NM, Lally KP. The CDH Study Group and advances in the clinical care of the patient with congenital diaphragmatic hernia. *Semin Perinatol* 2004;28:174–84.
- [2] Kimura O, Furukawa T, Higuchi K, et al. Impact of our new protocol on the outcome of the neonates with congenital diaphragmatic hernia. *Pediatr Surg Int* 2013;29:335–9.
- [3] Harrison MR, Keller RL, Hawgood SB, et al. A randomized trial of fetal endoscopic tracheal occlusion for severe fetal congenital diaphragmatic hernia. *N Engl J Med* 2003;349:1916–24.
- [4] Erspamer V. Amphibian skin peptides in mammals: looking ahead. *Trends Neurosci* 1983;6:200–1.
- [5] McDonald TJ, Jornvall H, Nilsson G, et al. Characterization of a gastrin-releasing peptide from porcine non-antral gastric tissue. *Biochem Biophys Res Commun* 1979;90:227–33.
- [6] Furukawa T, Kimura O, Go S, et al. Small bowel allografts maintained by administration of bombesin while under immunosuppression. *J Pediatr Surg* 2003;38:83–7.
- [7] Kinoshita H, Kimura O, Furukawa T, et al. Preoperative bombesin administration can protect the rat small bowel allograft from ischemic reperfusion injury. *J Pediatr Surg* 2005;40:1877–80.
- [8] Kimura O, Higuchi K, Furukawa T, et al. Neuroendocrine-immune modulation may be useful for allograft-specific immunosuppression in small bowel transplantation. *Transplant Proc* 2006;38:1825–6.
- [9] Higuchi K, Kimura O, Furukawa T, et al. Bombesin can rescue the enteric ganglia from FK506 neurotoxicity on small bowel transplantation. *J Pediatr Surg* 2006;41:1957–61.
- [10] Higuchi K, Kimura O, Furukawa T, et al. Bombesin can minimize impairments of interstitial cells of Cajal induced by FK506 in small bowel transplantation. *J Pediatr Surg* 2009;44:541–5.
- [11] Sunday ME, Hua J, Dai HB, et al. Bombesin increases fetal lung growth and maturation *in utero* and in organ culture. *Am J Respir Cell Mol Biol* 1990;3:199–205.
- [12] Sunday ME, Hua J, Reyes B, et al. Anti-bombesin antibodies modulate fetal mouse lung growth and maturation *in utero* and in organ cultures. *Anat Rec* 1993;236:25–32.
- [13] Sunday ME, Hua J, Torday J, et al. CD10/neutral endopeptidase 24.11 in developing human fetal lung: patterns of expression and modulation of peptide-mediated proliferation. *J Clin Invest* 1992;90:2517–25.
- [14] Wharton J, Polak JM, Bloom SR, et al. Bombesin-like immunoreactivity in the lung. *Nature* 1978;273:769–70.
- [15] Morikawa Y, Fujii K, Okada T, et al. Quantitative changes of lung tissue components during perinatal period in rats. *J Vet Med Sci* 1999;61:1229–33.
- [16] Fujino N, Kubo H, Suzuki T, et al. Isolation of alveolar epithelial type II progenitor cells from adult human lungs. *Lab Invest* 2011;91:363–78.
- [17] Suen HC, Bloch KD, Donahoe PK. Antenatal glucocorticoid corrects pulmonary immaturity in experimentally induced congenital diaphragmatic hernia in rats. *Pediatr Res* 1994;35:523–9.
- [18] Lally KP, Bagolan P, Hosie S, et al. Corticosteroids for fetuses with congenital diaphragmatic hernia: can we show benefit? *J Pediatr Surg* 2006;41:668–74.
- [19] Doi T, Sugimoto K, Rutenstock E, et al. Prenatal retinoic acid upregulates pulmonary gene expression of PI3K and AKT in nitrofen-induced pulmonary hypoplasia. *Pediatr Surg Int* 2010;26:1011–5.
- [20] Rutenstock EM, Doi T, Dingemann J, et al. Prenatal retinoic acid treatment upregulates late gestation lung protein 1 in the nitrofen-induced hypoplastic lung in late gestation. *Pediatr Surg Int* 2011;27:125–9.
- [21] Rutenstock E, Doi T, Dingemann J, et al. Prenatal administration of retinoic acid upregulates insulin-like growth factor receptors in the nitrofen-induced hypoplastic lung. *Birth Defects Res B Dev Reprod Toxicol* 2011;92:148–51.
- [22] Montedonico S, Sugimoto K, Felle P, et al. Prenatal treatment with retinoic acid promotes pulmonary alveologenesis in the nitrofen model of congenital diaphragmatic hernia. *J Pediatr Surg* 2008;43:500–7.
- [23] Gonzalez-Reyes S, Martinez L, Martinez-Calonge W, et al. Effects of antioxidant vitamins on molecular regulators involved in lung hypoplasia induced by nitrofen. *J Pediatr Surg* 2006;41:1446–52.
- [24] Kubota Y, Shimotake T, Iwai N. Congenital anomalies in mice induced by etretinate. *Eur J Pediatr Surg* 2000;10:248–51.
- [25] Takayasu H, Nakazawa N, Montedonico S, et al. Impaired alveolar epithelial cell differentiation in the hypoplastic lung in nitrofen-induced congenital diaphragmatic hernia. *Pediatr Surg Int* 2007;23:405–10.

# Immunosuppressive therapy with horse anti-thymocyte globulin and cyclosporine as treatment for fulminant aplastic anemia in children

Hiroshi Yagasaki · Hiroyuki Shichino · Akira Ohara · Ryoji Kobayashi · Hiromasa Yabe · Shouichi Ohga · Kazuko Hamamoto · Yoshitoshi Ohtsuka · Hiroyuki Shimada · Masami Inoue · Hideki Muramatsu · Yoshiyuki Takahashi · Seiji Kojima

Received: 19 July 2013 / Accepted: 2 December 2013 / Published online: 14 December 2013  
© Springer-Verlag Berlin Heidelberg 2013

**Abstract** Patients with severe aplastic anemia (SAA) and an absolute neutrophil count (ANC) of 0 typically have fatal outcomes. We defined fulminant AA (FAA) as ANC=0 for at least 2 weeks prior to and after immunosuppressive therapy (IST). We analyzed the outcomes of 35 children with FAA among 288 children who enrolled in a prospective study for AA (AA-97 study). AA was classified as FAA ( $n=35$ ), very SAA (vSAA;  $n=129$ ), or SAA ( $n=124$ ). All of the children received the IST with horse anti-thymocyte globulin (ATG) and cyclosporine (CsA). A significantly lower response rate at 6 months was seen in children with FAA when compared to those with vSAA or SAA (40.0, 63.6, and 63.7 %, respectively;  $p=0.027$ ). Of 20 nonresponder patients in the FAA group, 11 were rescued by alternative donor transplantation, and 5 patients showed a late response after 6 months. Consequently, no significant difference was noted in overall survival when comparing the FAA, vSAA, and SAA groups (88.5, 95.8, and 96.8 %). These findings indicate that IST with ATG and CsA

is justified as a first-line treatment for children with FAA who lack a human leukocyte antigen-matched sibling donor.

**Keywords** Children · Cyclosporine · Fulminant aplastic anemia · Horse anti-thymocyte globulin · Immunosuppressive therapy

## Introduction

Aplastic anemia (AA) is characterized by peripheral blood pancytopenia and bone marrow hypoplasia. Previously, the severe form of AA (SAA) was almost universally fatal. However, the prognosis of SAA has improved markedly in response to the introduction of immunosuppressive therapy (IST) with anti-thymocyte globulin (ATG) and cyclosporine (CsA) in the 1980s [1, 2]. In AA patients, survival after ATG therapy is dependent on the severity of the disease and

H. Yagasaki (✉) · H. Shichino  
Department of Pediatrics, School of Medicine, Nihon University,  
30-1 Ohyaguchi-Kamicho, Itabashi-ku 173-8610, Tokyo, Japan  
e-mail: yagasaki.hiroshi@nihon-u.ac.jp

A. Ohara  
Division of Blood Transfusion, Toho University Omori Hospital,  
Tokyo, Japan

R. Kobayashi  
Department of Pediatrics, Sapporo Hokuyu Hospital, Sapporo, Japan

H. Yabe  
Department of Cell Transplantation and Regenerative Medicine,  
Tokai University School of Medicine, Isehara, Japan

S. Ohga  
Department of Perinatal and Pediatric Medicine, Graduate School of  
Medical Sciences, Kyushu University, Fukuoka, Japan

K. Hamamoto  
Department of Pediatrics, Hiroshima Red Cross Hospital, Hiroshima,  
Japan

Y. Ohtsuka  
Department of Pediatrics, Hyogo College of Medicine, Hyogo, Japan

H. Shimada  
Department of Pediatrics, School of Medicine, Keio University,  
Tokyo, Japan

M. Inoue  
Department of Hematology/Oncology, Osaka Medical Center and  
Research Institute for Maternal and Child Health, Izumi City, Osaka,  
Japan

H. Muramatsu · Y. Takahashi · S. Kojima  
Department of Pediatrics, Graduate School of Medicine, Nagoya  
University, Nagoya, Japan

neutrophil counts [3]. Indeed, survival of AA patients with absolute neutrophil count (ANC) of  $<0.2 \times 10^9/L$  was significantly lower than that of AA patients with a neutrophil count of  $0.2$  to  $0.5 \times 10^9/L$  (23 vs. 61 %,  $p=0.01$ ) [4]. Further, in an analysis from the European Group for Blood and Marrow Transplantation (EBMT), the actuarial 5-year survival rates were 46 % in patients with ANC of  $<0.2 \times 10^9/L$  and 61 % in patients with ANC of  $0.2$  to  $0.5 \times 10^9/L$  [5]. SAA was originally defined as ANC of  $<0.5 \times 10^9/L$  by Camitta et al. [6]. Subsequently, Bacigalupo et al. proposed further subclassification into very SAA (vSAA) (ANC of  $<0.2 \times 10^9/L$ ) and SAA (ANC of  $0.2$  to  $0.5 \times 10^9/L$ ) [7]. Over the past decade, several studies have examined the relationship between disease severity and the response rate to IST or survival rate with varying results. For example, a German pediatric study showed a significantly better complete response (CR) rate and survival in patients with vSAA than those with SAA (68 vs. 45 %,  $p=0.009$ , and 93 vs. 81 %,  $p<0.001$ , respectively) [8]. In contrast, the Japanese AA-97 study showed comparable response rates at 6 months after IST in patients with vSAA and in patients with SAA (72 and 66 %, respectively) [9]. Several recent large studies reported that the severity of the disease or neutrophil counts at diagnosis did not predict the response to IST [10–12].

We experienced several cases of patients with an ANC of 0 and complete aplasia of bone marrow at the time of diagnosis. These patients had a particularly high risk of developing life-threatening infections. We designated these patients as having fulminant AA (FAA), defined as AA patients in whom ANC of 0 persist for more than 2 weeks prior to or after IST. We were not able to find any studies that had previously examined the clinical outcomes of the patients with FAA.

This study retrospectively analyzed the outcome of 35 patients with FAA who were enrolled in a prospective multicenter study for AA children.

## Patients and methods

**Patients and study design** From October 1997 to August 2009, a total of 288 patients with SAA (168 boys and 120 girls) were enrolled in the AA-97 study conducted by the Japan Childhood Aplastic Anemia Study Group. Among these patients, 205 who were enrolled in the study until April 2004 were already described in previous reports [13]. All were less than 18 years old and newly diagnosed with AA ( $\leq 180$  days from the time of diagnosis) without specific prior treatment. SAA was diagnosed if at least two of the following criteria were fulfilled: ANC of  $<0.5 \times 10^9/L$ , platelet count of  $<20 \times 10^9/L$ , or reticulocyte count of  $<20 \times 10^9/L$  with hypocellular bone marrow [6]. vSAA was diagnosed if the criteria for severe disease were fulfilled and if the ANC was  $<0.2 \times 10^9/L$  [7]. We defined FAA as ANC=0 for at least 2 weeks prior to and after IST. The study protocol was approved by the ethics committee of each participating hospital and conformed to the recently revised Declaration of Helsinki. Written informed consent was obtained from all parents, and all patients over the age of 10 years agreed to participate in the study.

All patients were treated with a combination of intravenous horse ATG (Lymphoglobulin; Genzyme, Cambridge, USA) at 15 mg/kg/day for 5 days and oral CsA at 6 mg/kg/day. The dose of CsA was adjusted to maintain trough levels between 100 and 200 ng/mL, and an appropriate dose was administered for at least 6 months. Granulocyte colony-stimulating factor (filgrastim; Kirin, Tokyo, Japan) was administered intravenously or subcutaneously at 400  $\mu\text{g}/\text{m}^2$  for 3 months only to patients with ANC of  $<0.2 \times 10^9/L$ .

CR was defined as ANC of  $>1.5 \times 10^9/L$ , platelet count of  $>100 \times 10^9/L$ , and hemoglobin (Hb) level of  $>11.0$  g/dL. Partial response (PR) was defined as ANC of  $>0.5 \times 10^9/L$ , platelet count of  $>20 \times 10^9/L$ , and Hb level of  $>8.0$  g/dL. The overall response rate (RR) was defined as CR or PR at 3 and

**Table 1** Patient characteristics

	FAA	vSAA	SAA
Patient number	35	129	124
Sex (male/female)	15/20	83/46	70/54
Median age, years (range)	11 (0–16)	8 (0–16)	9 (0–16)
Cause of aplastic anemia			
Idiopathic	25	104	105
Hepatitis	8	22	17
Drug	2	3	2
Median days from diagnosis to treatment (range)	15 (0–77)	14 (0–102)	18 (1–180)
Median WBC count $\times 10^9/L$ (range)*	1.4 (0.2–8.5)	1.7 (0.2–5.8)	2.2 (0.4–6.1)
Median neutrophil count $\times 10^9/L$ (range)	0	0.11 (0.01–0.19)	0.35 (0.2–0.93)
Median reticulocyte count $\times 10^9/L$ (range)*	3 (0–33)	8 (0–83)	25 (0–202)
Median platelet count $\times 10^9/L$ (range)*	6 (1–11)	7 (1–43)	11 (1–52)
Median observation time, months (range)	83 (5–147)	80 (11–158)	85 (1–180)

FAA fulminant aplastic anemia,  
vSAA very severe aplastic anemia,  
SAA severe aplastic anemia,  
WBC white blood cell

\* $p<0.05$ , statistically significant

**Table 2** Response to treatment

	FAA	vSAA	SAA
3 months			
Evaluable number	35	129	123
CR	1	9	14
PR	6	50	54
NR	28	70	55
	20%	45.7%	54.8%
6 months			
Evaluable number	34	129	122
CR	5	21	30
PR	9	61	49
NR	20	47	43
	40.0%	63.6%	63.7%

FAA fulminant aplastic anemia, vSAA very severe aplastic anemia, SAA severe aplastic anemia

6 months after IST. Failure-free survival (FFS) was defined as survival without treatment failure, which was the first event following IST, including death from any cause, need for secondary treatment [second IST or stem cell transplantation (SCT)], relapse, and clonal evolution to acute myeloid leukemia/myelodysplastic syndrome (AML/MDS) or paroxysmal nocturnal hemoglobinuria (PNH).

**Statistical analysis** Overall survival (OS) and FFS were calculated using the Kaplan–Meier method. The difference was analyzed with the log-rank test. RR was compared using the  $\chi^2$  test. A value of  $p < 0.05$  was considered statistically significant. All analyses were conducted using R version 2.11.1 software.

## Results

### Baseline characteristics

Patient profiles are shown in Table 1. Patients were classified into the following three groups according to disease severity: 35 with FAA, 129 with vSAA, and 124 with SAA. Median age at diagnosis was 11 years in the FAA group, 8 years in the vSAA group, and 9 years in the SAA group. Median interval between diagnosis and treatment was 15, 14, and 18 days, respectively. Median follow-up at the time of analysis was 83, 80, and 85 months, respectively.

### Treatment response

Of the 288 patients, 134 (46.5 %) and 175 (60.8 %) achieved CR or PR at 3 and 6 months after IST, respectively. Subgroup analyses revealed that RR at 3 and 6 months was significantly

lower in the FAA group than in the vSAA and SAA groups (20.0, 45.7, and 54.8 % at 3 months, respectively,  $p = 0.001$ ; 40.0, 63.6, and 63.7 % at 6 months, respectively,  $p = 0.027$ ) (Table 2). These results indicate that FAA was associated with significantly poorer RR to IST than vSAA and SAA.

### Outcomes of nonresponders and failure-free survival

The clinical outcomes of nonresponders in each group are shown in Table 3. Of 20 nonresponders in the FAA group, 5 patients achieved a late response, and 15 patients had either one of treatment failure as follows: clonal evolution ( $n = 4$ ), need for second IST ( $n = 2$ ), or SCT ( $n = 9$ ). Of 14 responders, two patients had the following treatment failure: relapse ( $n = 1$ ) and need for SCT ( $n = 1$ ). Because one patient had an early death, the total number of treatment failure was 18 in the FAA group.

Of 47 nonresponders in the vSAA group, nine patients achieved a late response, and three patients were alive without response. Therefore, 35 patients had either one of treatment failure as follows: death ( $n = 1$ ), need for second IST ( $n = 12$ ), or SCT ( $n = 22$ ). Of 82 responders, 12 patients had the following treatment failure: clonal evolution ( $n = 2$ ), relapse ( $n = 8$ ), need for second IST ( $n = 1$ ), or SCT ( $n = 1$ ). Therefore, the total number of treatment failure was 47 in the vSAA group.

Of 43 nonresponders in the SAA group, nine patients achieved a late response, and two patients were alive without response. One patient with a delayed response relapsed thereafter. Totally, 33 patients had either one of treatment failure as follows: clonal evolution ( $n = 3$ ), relapse ( $n = 1$ ), need for second IST ( $n = 11$ ), or SCT ( $n = 18$ ). Of 79 responders, eight patients had the following treatment failure: clonal evolution ( $n = 1$ ), relapse ( $n = 4$ ), and need for second IST ( $n = 3$ ).

**Table 3** Clinical course of nonresponders; second line and 3rd line treatments

Second-line therapy	No.	Outcome	No.	Third-line therapy	No.	Outcome	No.
<b>FAA</b>							
None	9	Late response/alive	5				
		Evolution to overt leukemia	4	UBMT	1	Alive	1
				UCBT	3	Dead	3
Second IST	2	No response	2	None	1	Alive	1
				MR-BMT	1	Alive	1
U/MR-BMT	8	Alive	8				
UCBT	1	Alive	1				
<b>vSAA</b>							
None	13	Late response/alive	9				
		No response	4	None	4	Alive	3
						Dead	1
Second IST	12	Response/alive	4				
		No response	8	None	3	Alive	3
				U/MR-BMT	5	Alive	5
U/MR-BMT	21	Alive	17				
		Dead	3				
		Rejection	1	UCBT	1	Alive	1
UCBT	1	Alive					
<b>SAA</b>							
None	14	Late response/alive	8				
		Late response but relapse	1	None		Alive	1
		No response	2	None	2	Alive	2
		Evolution to overt leukemia	3	UBMT	3	Alive	3
Second IST	11	Response/alive	3				
		No response	8	UBMT	4	Alive	4
				UCBT	1	Alive	1
				None	3	Alive	1
						Dead	2
U/MR-BMT	18	Alive	15				
		Dead	2				
		Rejection	1	UCBT	1	Alive	1

FAA fulminant aplastic anemia, vSAA very severe aplastic anemia, SAA severe aplastic anemia, IST immunosuppressive therapy, UBMT unrelated donor bone marrow transplantation, MR-BMT mismatched related donor bone marrow transplantation, UCBT unrelated cord blood transplantation

Because two patients had an early death, the total number of treatment failure was 43 in the SAA group.

As a result, the 5-year FFS is 48.2 % [95 % confidence interval (CI), 34.1–68.2 %] in the FAA group, 65.1 % (95 % CI, 57.3–74.1 %) in the vSAA group, and 68.1 % (95 % CI, 60.3–77.0 %) in the SAA group, respectively (Fig. 1a). This difference was not significant ( $p=0.206$ ).

#### Overall survival and causes of death

As indicated in Table 3, 11 of 20 nonresponders in the FAA group were rescued by SCT, and 5 achieved a late response. Of 47 nonresponders in the vSAA group, 24 were rescued by

SCT, and 9 achieved a late response. Of 43 nonresponders in the SAA group, 24 were rescued by SCT, and 9 achieved a late response. Both alternative donor SCT and late response substantially raised the OS in all three groups. The 5-year OS was comparable among the three groups: 88.5 % in the FAA group (95 % CI, 78.5–99.8 %), 95.8 % in the vSAA group (95 % CI, 92.2–99.5 %), and 96.8 % in the SAA group (95 % CI, 93.7–99.9 %), respectively ( $p=0.281$ ) (Fig. 1b). A total of 16 patients died of the following causes: sepsis ( $n=3$ ), evolution to overt leukemia ( $n=3$ ), transplantation-related toxicities ( $n=7$ ), and other causes ( $n=3$ ). The causes of death in each group are shown in Table 4. It is noteworthy that only one patient died of infection among the 35 patients with FAA.

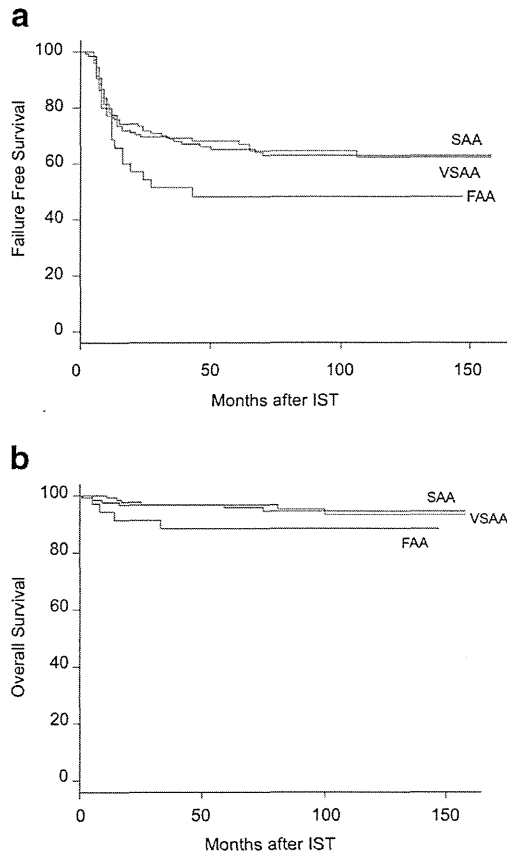


**Fig. 1** The 5-year FFS (a) and the 5-year OS (b) according to the severity of AA. The 5-year FFS was 48.2 % in the FAA group, 65.1 % in the vSAA group, and 68.1 % in the SAA group, respectively. However, no significant difference was demonstrated ( $p=0.206$ ). The 5-year OS was comparable among the three groups: 88.5 % in the FAA group, 95.8 % in the vSAA group, and 96.8 % in the SAA group, respectively

**Discussion**

The current study showed that the trilineage hematologic recovery was seen in 40 % of FAA patients, which was significantly inferior to the rate of recovery seen in those with

vSAA and SAA. However, the OS reached 88.5 % in the FAA group, which was comparable to the OS seen in the other two groups. The ability to maintain patients alive with persistent neutropenia and high success of alternative donor SCT might contribute to the favorable survival. Indeed, only one patient died of infectious complications among the FAA patients. According to a report from the National Institutes of Health, infection-related mortality decreased from 37 % in the early 1990s to 11 % in the 2000s among nonresponders to IST [14]. Because granulocyte colony-stimulating factor is not effective in increasing neutrophil counts of patients with FAA [15, 16], the improvement of survival may be mainly attributable to advances of anti-infectious agents, especially antifungal drugs.

Another reason for the favorable OS in this study is the young age of the patient population. In multivariate analysis, age of <16 years is a significantly favorable factor for the OS in SAA patients who receive IST. Indeed, the OS was 100, 92, 71, and 60 % for patients <20, 20–40, 40–60, and >60 years of age, respectively, in a recent European study [17]. Due to the higher number of deaths that occurs before treatment response in older patients, they are more likely to be nonresponders than younger patients.

Outcomes after unrelated donor BMT (UBMT) for children with SAA have resulted in marked improvements and are now similar to those after matched sibling donor BMT [18–20]. Therefore, several investigators advocate UBMT as the first-line treatment for SAA children who lack a matched sibling donor. However, it takes more than 3 months to find a suitable unrelated donor through the marrow donor bank in Japan. Other alternative donor transplantations, including unrelated cord blood transplantation (UCBT) and haploidentical transplantation from a family donor, can reduce the time needed to find a suitable donor.

Although UCBT has been used for SAA, the results are not encouraging. The Japan Cord Blood Bank Network analyzed the outcome of 31 SAA patients who received UCBT. As a result, the 2-year OS was 41 % [21]. Forty-five patients with SAA who received UCBT as their first transplant were reported to the Center for International Blood and Marrow Transplant Research. The observed graft failure rate was 30 %, and the 2-year OS was 35 % [22]. On the other hand, several successful case series of haploidentical SCT with or without T cell depletion were also reported [23, 24]. However, the results of these studies were too limited to determine whether haploidentical SCT should be employed as a first-line therapy.

Accordingly, at present, IST with ATG and CsA is justified as a first-line treatment for children with FAA who lack a matched sibling donor.

**Table 4** Causes of death

FAA	vSAA	SAA
Sepsis ( $n=1$ )	Sepsis ( $n=1$ )	Sepsis ( $n=1$ )
Transplantation-related toxicities ( $n=1$ )	Transplantation-related toxicities ( $n=4$ )	Transplantation-related toxicities ( $n=2$ )
Evolution to overt leukemia ( $n=2$ )	Evolution to overt leukemia ( $n=1$ )	Hemolysis ( $n=1$ )
		Accident ( $n=1$ )
		Hemochromatosis ( $n=1$ )

FAA fulminant aplastic anemia, vSAA very severe aplastic anemia, SAA severe aplastic anemia

**Conflict of interest** The authors report no competing interests.



## References

- Frickhofen N, Kaltwasser JP, Schrezenmeier H, Raghavachar A, Vogt HG, Herrmann F, Freund M, Meusers P, Salama A, Heimpel H (1991) Treatment of aplastic anemia with antilymphocyte globulin and methylprednisolone with or without cyclosporine. The German Aplastic Anemia Study Group. *N Engl J Med* 324:1297–1304
- Rosenfeld SJ, Kimball J, Vining D, Young NS (1995) Intensive immunosuppression with antithymocyte globulin and cyclosporine as treatment for severe acquired aplastic anemia. *Blood* 85:3058–3065
- Gluckman E, Devergie A, Poros A, Degoulet P (1982) Results of immunosuppression in 170 cases of severe aplastic anaemia. Report of the European Group of Bone Marrow Transplant (EGBMT). *Br J Haematol* 51:541–550
- Marsh JC, Hows JM, Bryett KA, Al-Hashimi S, Fairhead SM, Gordon-Smith EC (1987) Survival after antilymphocyte globulin therapy for aplastic anemia depends on disease severity. *Blood* 70:1046–1052
- Bacigalupo A, Hows J, Gluckman E, Nissen C, Marsh J, Van Lint MT, Congiu M, De Planque MM, Ernst P, McCann S et al (1988) Bone marrow transplantation (BMT) versus immunosuppression for the treatment of severe aplastic anaemia (SAA): a report of the EBMT SAA working party. *Br J Haematol* 70:177–182
- Camitta BM, Thomas ED, Nathan DG, Gale RP, Kopecky KJ, Rapoport JM, Santos G, Gordon-Smith EC, Storb R (1979) A prospective study of androgens and bone marrow transplantation for treatment of severe aplastic anemia. *Blood* 53:504–514
- Bacigalupo A, Chaple M, Hows J, Van Lint MT, McCann S, Milligan D, Chessells J, Goldstone AH, Ottolander J, Van't Veer ET et al (1993) Treatment of aplastic anaemia (AA) with antilymphocyte globulin (ALG) and methylprednisolone (MPred) with or without androgens: a randomized trial from the EBMT SAA working party. *Br J Haematol* 83:145–151
- Führer M, Rampf U, Baumann I, Faldum A, Niemyer C, Janka-Schaub G, Friedrich W, Ebell W, Borkhardt A, Bender-Goetze C (2005) Immunosuppressive therapy for aplastic anemia in children: a more severe disease predicts better survival. *Blood* 106:2102–2104
- Kosaka Y, Yagasaki H, Sano K, Kobayashi R, Ayukawa H, Kaneko T, Yabe H, Tsuchida M, Mugishima H, Ohara A, Morimoto A, Otsuka Y, Ohga S, Bessho F, Nakahata T, Tsukimoto I, Kojima S, Japan Childhood Aplastic Anemia Study Group (2008) Prospective multicenter trial comparing repeated immunosuppressive therapy with stem-cell transplantation from an alternative donor as second-line treatment for children with severe and very severe aplastic anemia. *Blood* 111:1054–1059
- Scheinberg P, Wu CO, Nunez O, Young NS (2009) Predicting response to immunosuppressive therapy and survival in severe aplastic anaemia. *Br J Haematol* 144:206–216. doi:10.1111/j.1365-2141.2008.07450.x
- Locasciulli A, Oneto R, Bacigalupo A, Socié G, Korthof E, Bekassy A, Schrezenmeier H, Passweg J, Führer M, Severe Aplastic Anemia Working Party of the European Blood and Marrow Transplant Group (2007) Outcome of patients with acquired aplastic anemia given first line bone marrow transplantation or immunosuppressive treatment in the last decade: a report from the European Group for Blood and Marrow Transplantation (EBMT). *Haematologica* 92:11–18
- Yoshida N, Yagasaki H, Hama A, Takahashi Y, Kosaka Y, Kobayashi R, Yabe H, Kaneko T, Tsuchida M, Ohara A, Nakahata T, Kojima S (2011) Predicting response to immunosuppressive therapy in childhood aplastic anemia. *Haematologica* 96:771–774. doi:10.3324/haematol.2010.032805
- Kojima S, Hibi S, Kosaka Y, Yamamoto M, Tsuchida M, Mugishima H, Sugita K, Yabe H, Ohara A, Tsukimoto I (2000) Immunosuppressive therapy using antithymocyte globulin, cyclosporine, and danazol with or without human granulocyte colony-stimulating factor in children with acquired aplastic anemia. *Blood* 96:2049–2054
- Valdez JM, Scheinberg P, Nunez O, Wu CO, Young NS, Walsh TJ (2011) Decreased infection-related mortality and improved survival in severe aplastic anemia in the past two decades. *Clin Infect Dis* 52:726–735. doi:10.1093/cid/ciq245
- Kojima S, Fukuda M, Miyajima Y, Matsuyama T, Horibe K (1991) Treatment of aplastic anemia in children with recombinant human granulocyte colony-stimulating factor. *Blood* 77:937–941
- Kojima S, Matsuyama T (1994) Stimulation of granulopoiesis by high-dose recombinant human granulocyte colony-stimulating factor in children with aplastic anemia and very severe neutropenia. *Blood* 83:1474–1478
- Tichelli A, Schrezenmeier H, Socié G, Marsh J, Bacigalupo A, Dührsen U, Franzke A, Hallek M, Thiel E, Wilhelm M, Höchsmann B, Barrois A, Champion K, Passweg JR (2011) A randomized controlled study in patients with newly diagnosed severe aplastic anemia receiving antithymocyte globulin (ATG), cyclosporine, with or without G-CSF: a study of the SAA Working Party of the European Group for Blood and Marrow Transplantation. *Blood* 117:4434–4441. doi:10.1182/blood-2010-08-304071
- Kennedy-Nasser AA, Leung KS, Mahajan A, Weiss HL, Arce JA, Gottschalk S, Carrum G, Khan SP, Heslop HE, Brenner MK, Bollard CM, Krance RA (2006) Comparable outcomes of matched-related and alternative donor stem cell transplantation for pediatric severe aplastic anemia. *Biol Blood Marrow Transplant* 12:1277–1284
- Yagasaki H, Takahashi Y, Hama A, Kudo K, Nishio N, Muramatsu H, Tanaka M, Yoshida N, Matsumoto K, Watanabe N, Kato K, Horibe K, Kojima S (2010) Comparison of matched-sibling donor BMT and unrelated donor BMT in children and adolescent with acquired severe aplastic anemia. *Bone Marrow Transplant* 45:1508–1513. doi:10.1038/bmt.2009.378
- Marsh JC, Bacigalupo A, Schrezenmeier H, Tichelli A, Risitano AM, Passweg JR, Killick SB, Warren AJ, Foukaneli T, Aljurf M, Al-Zahrani HA, Schafhausen P, Roth A, Franzke A, Brummendorf TH, Dufour C, Oneto R, Sedgwick P, Barrois A, Kordasti S, Elebute MO, Mufti GJ, Socié G, European Blood and Marrow Transplant Group Severe Aplastic Anaemia Working Party (2012) Prospective study of rabbit antithymocyte globulin and cyclosporine for aplastic anemia from the EBMT Severe Aplastic Anaemia Working Party. *Blood* 119:5391–5396. doi:10.1182/blood-2012-02-407684
- Yoshimi A, Kojima S, Taniguchi S, Hara J, Matsui T, Takahashi Y, Azuma H, Kato K, Nagamura-Inoue T, Kai S, Kato S, Japan Cord Blood Bank Network (2008) Unrelated cord blood transplantation for severe aplastic anemia. *Biol Blood Marrow Transplant* 14:1057–1063. doi:10.1016/j.bbmt.2008.07.003
- Eapen M, Horowitz MM (2010) Alternative donor transplantation for aplastic anemia. *Hematology Am Soc Hematol Educ Program* 2010:43–46. doi:10.1182/asheducation-2010.1.43
- Xu LP, Liu KY, Liu DH, Han W, Chen H, Chen YH, Zhang XH, Wang Y, Wang FR, Wang JZ, Huang XJ (2012) A novel protocol for haploidentical hematopoietic SCT without in vitro T-cell depletion in the treatment of severe acquired aplastic anemia. *Bone Marrow Transplant* 47:1507–1512. doi:10.1038/bmt.2012.79
- Im HJ, Koh KN, Choi ES, Jang S, Kwon SW, Park CJ, Chi HS, Seo JJ (2013) Excellent outcome of haploidentical hematopoietic stem cell transplantation in children and adolescents with acquired severe aplastic anemia. *Biol Blood Marrow Transplant* 19:754–759. doi:10.1016/j.bbmt.2013.01.023

Available at [www.sciencedirect.com](http://www.sciencedirect.com)

ScienceDirect

journal homepage: [www.ejcancer.com](http://www.ejcancer.com)

## Novel 1p tumour suppressor Dnmt1-associated protein 1 regulates MYCN/ataxia telangiectasia mutated/p53 pathway



Yohko Yamaguchi<sup>a</sup>, Hisanori Takenobu<sup>a</sup>, Miki Ohira<sup>b</sup>, Atsuko Nakazawa<sup>c</sup>, Sayaka Yoshida<sup>a</sup>, Nobuhiro Akita<sup>a</sup>, Osamu Shimozato<sup>a</sup>, Atsushi Iwama<sup>d</sup>, Akira Nakagawara<sup>e</sup>, Takehiko Kamijo<sup>a,\*</sup>

<sup>a</sup> Division of Biochemistry and Molecular Carcinogenesis, Chiba Cancer Center Research Institute, Japan

<sup>b</sup> Laboratory of Cancer Genomics, Chiba Cancer Center Research Institute, Japan

<sup>c</sup> Department of Pathology, National Center for Child Health and Development, Japan

<sup>d</sup> Department of Cellular and Molecular Medicine, Graduate School of Medicine, Chiba University, Chiba, Japan

<sup>e</sup> Division of Biochemistry and Innovative Cancer Therapeutics, Chiba Cancer Center Research Institute, Japan

Available online 19 February 2014

### KEYWORDS

DMAP1  
ATM  
p53  
Neuroblastoma  
MYCN

**Abstract** Neuroblastoma (NB) is a paediatric solid tumour which originates from sympathetic nervous tissues. Deletions in chromosome 1p are frequently found in unfavourable NBs and are correlated with v-myc avian myelocytomatosis viral oncogene neuroblastoma derived homolog (*MYCN*) amplification; however, it remains to be elucidated how the 1p loss contributes to MYCN-related oncogenic processes in NB. In this study, we identified the role of Dnmt1-associated protein 1 (DMAP1), coded on chromosome 1p34, in the processes. We studied the expression and function of DMAP1 in NB and found that low-level expression of DMAP1 related to poor prognosis, unfavourable histology and 1p Loss of heterozygosity (LOH) of primary NB samples. Intriguingly, DMAP1 induced ataxia telangiectasia mutated (ATM) phosphorylation and focus formation in the presence of a DNA damage reagent, doxorubicin. By DMAP1 expression in NB and fibroblasts, p53 was activated in an ATM-dependent manner and p53-downstream pro-apoptotic Bcl-2 family molecules were induced at the mRNA level, resulting in p53-induced apoptotic death. *BAX* and *p21<sup>Cip1/Waf1</sup>* promoter activity dependent on p53 was clearly up-regulated by DMAP1. Further, MYCN transduction in MYCN single-copy NB cells accelerated doxorubicin (Doxo)-induced apoptotic cell death; MYCN is implicated in DMAP1 protein stabilisation and ATM phosphorylation in these situations. DMAP1 knockdown attenuated MYCN-dependent ATM phosphorylation and NB cell apoptosis. Together, DMAP1

\* Corresponding author: Address: Division of Biochemistry and Molecular Carcinogenesis, Chiba Cancer Center Research Institute, 666-2 Nitona, Chuo-ku, Chiba 260-8717, Japan. Tel.: +81 43 264 5431; fax: +81 43 265 4459.

E-mail address: [tkamijo@chiba-cc.jp](mailto:tkamijo@chiba-cc.jp) (T. Kamijo).

<http://dx.doi.org/10.1016/j.ejca.2014.01.023>

0959-8049/© 2014 Elsevier Ltd All rights reserved.

appears to be a new candidate for a 1p tumour suppressor and its reduction contributes to NB tumourigenesis via inhibition of MYCN-related ATM/p53 pathway activation.

© 2014 Elsevier Ltd All rights reserved.

## 1. Introduction

Genetic and molecular analyses have indicated various types of deletions of the short arm of chromosome 1 (1p) in a broad range of human malignant tumours, including neuroblastoma (NB) and others [1–5]. It has been suggested that this genomic region harbours several tumour suppressor genes and that additive effects of loss of those tumour suppressors on tumourigenesis exist in several ‘1p loss malignant tumours’.

NB is the second most common paediatric solid malignant tumour derived from sympathetic nervous tissues. Extensive cytogenetic and molecular genetic studies have identified that genetic abnormalities, such as loss of the short arm of 1p, 11q and 14q; amplification of *MYCN*; and allelic gain of 11p and 17q, are frequently observed [1]. Deletion of the 1p region is highly correlated with both *MYCN* amplification and an adverse patient outcome, indicating the presence of several tumour suppressor genes (TSGs) within this region [6]. NB tumours with *MYCN* in a single copy had preferentially lost the 1p36 allele and these tumours also had a very distal commonly deleted region; in contrast, all *MYCN*-amplified NBs had larger 1p deletions, extending from the telomere to 1p31 [7]. The extent of deletion or LOH was identified in 184 primary NBs; in 80%, the 1p deletion extended from the telomere to 1p31 [8]. Given the tendency of large, hemizygous 1p deletions in *MYCN*-amplified NBs, alternative hypotheses for tumour suppression are: (1) an additional, *MYCN*-associated TSG in the 1p region; (2) suppression of TSG expression from a hemizygous allele due to epigenetic modifications except for imprinting, e.g. miRNAs and non-coding RNAs; (3) haplo-insufficiency-based suppression accounting for the rarity of 1p homozygous deletions [9].

Dnmt1-associated protein 1 (DMAP1) was originally identified as a molecule interacting with DNMT1 and was demonstrated to co-localise with PCNA and DNMT1 at DNA replication foci during the S phase [10]. Previously, we reported that Dmap1 participates in DNA repair and transformation of mouse embryonic fibroblasts (MEFs). Dmap1 was recruited to the damaged sites, formed complexes with  $\gamma$ -H2AX and directly interacted with Proliferating Cell Nuclear Antigen (Pcna); inhibition of this binding impaired the accumulation of the Pcna-Caf-1 complex at damaged sites and resulted in DNA breaks [11]. In addition, Penicud and Behrens reported that DMAP1 promotes ataxia telangiectasia mutated (ATM) recruitment and focus formation at damaged sites. These results suggest that DMAP1 is involved in the DNA damage response (DDR) [12]. Interestingly,

DMAP1 gene is coded in 1p34 and the region that is frequently deleted in NB tumours with 1p LOH [8,9]. These results prompted us to study the expression level of DMAP1 in neuroblastoma samples and its functional role in tumourigenesis.

In the present report, for the first time, we found that DMAP1 is a novel 1p tumour suppressor and DMAP1 has an indispensable role in MYCN-related ATM/p53 pathway activation. Downregulation of DMAP1 seems to be a result of MYCN-induced stress and an important mechanism for NB tumourigenesis.

## 2. Materials and methods

### 2.1. Cell culture

Human NB cell lines were obtained from official cell banks (RIKEN Bioresource Cell Bank, Tohoku University Cell Resource Center, and the American Type Culture Collection) and were cultured in RPMI1640 or Dulbecco's modified Eagle's medium (Wako, Osaka, Japan) supplemented with 10% heat-inactivated foetal bovine serum (Invitrogen, Carlsbad, CA, United States of America (USA)) and 50  $\mu$ g/ml penicillin/streptomycin (Sigma–Aldrich, St. Louis, MO, USA) in an incubator with humidified air at 37 °C with 5% CO<sub>2</sub>. ATM kinase inhibitor, KU-55933 (Santa Cruz Biotechnology, Santa Cruz, CA, USA) was dissolved in DMSO to make stock solutions of 20 mM.

### 2.2. Lentiviral production and infection for over-expression and knockdown of genes

For the over-expression of mouse Dmap1 and human DMAP1, cDNAs were subcloned into lentiviral vector pHR-SIN-CSGW [13]. For shRNA-based knockdown experiments, pLKO.1 puromycin-based lentiviral vectors containing five sequence-verified shRNAs targeting human DMAP1 (RefSeq NM\_019100.4, NM\_001034024.1, NM\_001034023.1) were obtained from the MISSION TRC-Hs 1.0 Human, shRNA library (Sigma–Aldrich). We checked DMAP1 knockdown by five lentivirus-produced shRNAs (clones: TRCN0000021744-21748) and used at least two shRNAs for experiments. Lentiviral production, infection and confirmation of infection efficiency were performed as described previously [13].

### 2.3. Antibodies

Antibodies against p53 (DO-1) and MYCN (rabbit polyclonal, C-19) were purchased from Santa Cruz Biotechnology. Antibodies against p53Ser15-P (rabbit

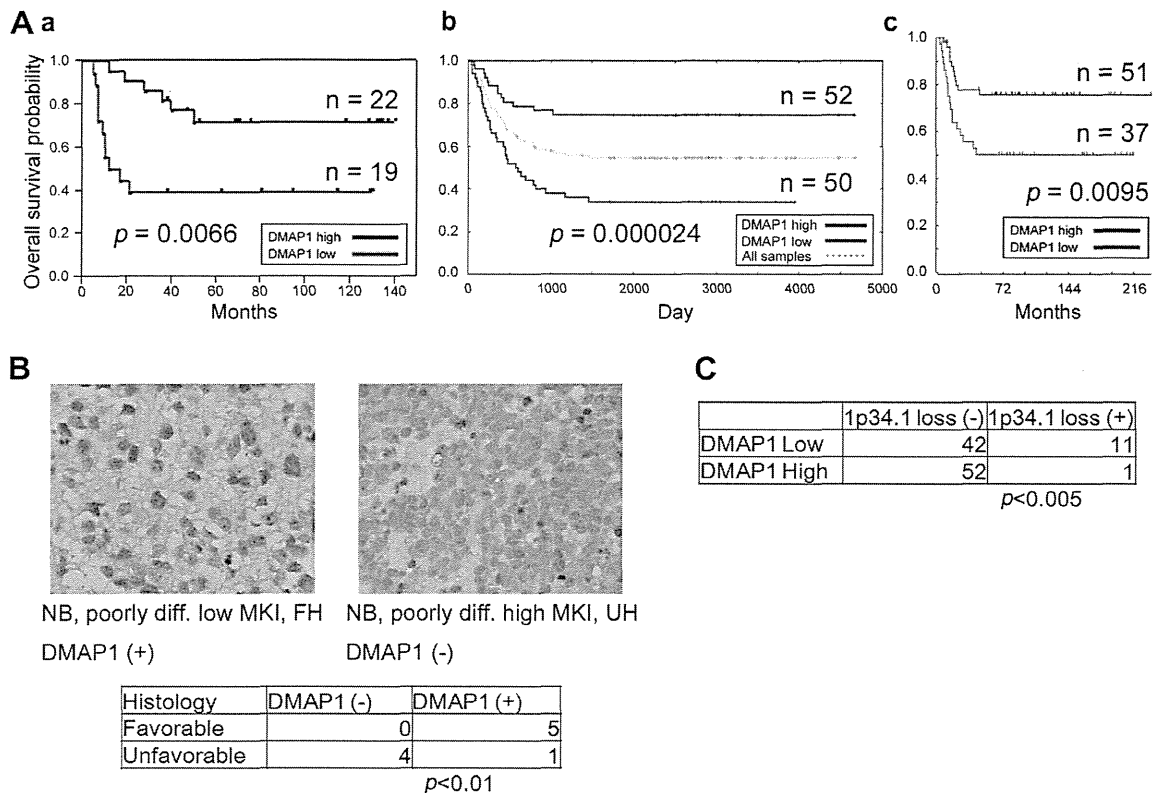


Fig. 1. Expression level of DMAP1 in neuroblastoma (NB) samples and neuroblastoma cell lines. (A) Kaplan–Meier survival analysis of NB patients based on higher or lower expression levels of *DMAP1* (overall survival analysis) presented by microarray analysis in three individual cohorts. (Aa) Chiba Cancer Center Research Institute cohort ( $n = 41$ ). Expression levels of *DMAP1* were separated into a high or low group based on the average expression. Statistical analysis was performed by the log-rank test. Corresponding  $p$  values are indicated. (Ab) Childrens Hospital Los Angeles cohort (<http://pob.abcc.ncifcrf.gov/cgi-bin/JK>), Neuroblastoma Prognosis Database–Seeger Lab dataset.  $n = 102$ . Expression levels of *DMAP1* on probe 224163\_s\_at were separated into a high or low group based on the median expression. (Ac) Academic Medical Center cohort R2 microarray analysis and visualisation platform (<http://r2.amc.nl>), Tumor Neuroblastoma public–Versteeg–88 dataset.  $n = 88$ . Expression levels of *DMAP1* on probe 224163\_s\_at were separated into a high or low group based on the expression cutoff value 118.0 according to the R2 algorithm. (B) Immunohistochemical staining for DMAP1 in NB. Statistical significance was determined by Fisher’s exact probability test. MKI: Mitosis-karyorrhexis index. FH: favourable histology; UH: unfavourable histology. DMAP1 (+): DMAP1 high-expression tumour; DMAP1 (–): DMAP1 low-expression tumour. (C) 1p loss was studied by array CGH analysis. Expression status of *DMAP1* was quantified by quantitative polymerase chain reaction (qPCR) analysis and normalised by *GAPDH* expression. *DMAP1* high or low expression was determined by its median value. Fisher’s exact probability test was applied to determine statistical significance.

polyclonal) and ATMSer1981-P (10H11, E12) were from Cell Signaling Technology (Danvers, MA, USA). Anti-ATM rabbit polyclonal antibody (Ab-3) was from Merck Millipore. Antibodies against  $\beta$ -Actin (rabbit polyclonal) and anti-FLAG (M2) were from Sigma–Aldrich. A mouse monoclonal anti-tubulin antibody was from Neomarkers Lab Vision (Fremont, CA, USA). Anti-DMAP1 rabbit polyclonal antibody (ab2848) was from Abcam (Cambridge, United Kingdom (UK)), anti-DMAP1 (2G12) was from Abnova (Taipei, Taiwan) and anti-human influenza hemagglutinin (HA) rabbit polyclonal was from MBL (Nagoya, Japan).

#### 2.4. Statistical analysis

All data were tested statistically using the Welch test and Fisher’s exact probability test.  $p < 0.05$  was considered to indicate statistical significance. Kaplan–Meier survival curves were calculated, and survival distributions

were compared using the log-rank test. Cox regression models were used to explore associations between *DMAP1* expression, age at diagnosis, tumour stage, *TrkA* expression, *MYCN* copy number, tumour origin, DNA ploidy, Shimada pathology and survival. Statistical significance was declared if  $p < 0.05$ . Statistical analysis was performed using JMP 8.0 (SAS Institute Inc., Cary, NC, USA).

Other methods are described in Supplementary information.

### 3. Results

#### 3.1. Low expression level of *DMAP1* correlated with unfavourable prognosis of NB patients

We examined the expression levels of *DMAP1* in NB samples by microarray analysis. Kaplan–Meier survival analysis showed that low *DMAP1* expression correlated

with the unfavourable prognosis of NB patients (Fig. 1Aa). Web-based microarray analysis and visualisation application for NB confirmed these results (Fig. 1Ab, c), and it was also shown by quantitative polymerase chain reaction (qPCR) (Suppl. Fig. S1Aa). Unfavourable NBs, which are classified by International Neuroblastoma Staging System (INSS) stage with *MYCN* copy number, also expressed low-level *DMAPI* (Suppl. Fig. S1B). Immunohistochemical analysis also showed low expression of *DMAPI* in unfavourable histology NB (Fig. 1B).

Next, the chromosome 1p status was analysed by array CGH to study the mechanism of *DMAPI* reduction in unfavourable NB (Fig. 1C). As a result, *DMAPI* reduction in unfavourable NB was significantly correlated with loss of its gene locus. *DMAPI* mRNA levels were significantly lower in NB cell lines than in primary NB samples (Suppl. Fig. S1C). To further assess other possibilities for the suppression of *DMAPI* expression, bisulphite sequencing was carried out using five clinical samples and two cell lines of NB and *BMII* knockdown to study epigenetic suppression by polycombs in NB cell lines; however, DNA methylation of the *DMAPI* promoter region and transcriptional suppression of *DMAPI* by *BMII* were not found (data not shown). Next, univariate Cox regression was employed to examine the individual relationship of each variable to survival (Table 1). These variables were: *DMAPI* expression, age at diagnosis (>1 year old versus <1 year old), tumour stage (3 + 4 versus 1 + 2 + 4s), *TrkA* expression (low versus high), *MYCN* copy number (amplified versus non-amplified), origin (adrenal gland versus others), DNA ploidy (aneuploidy versus di-/tetraploidy) and Shimada pathology (favourable versus unfavourable), all of which were found statistically to be of prognostic importance. Additionally, multivariable Cox analysis demonstrated that *DMAPI* expression was an independent prognostic factor from tumour origin, stage and DNA ploidy. However, the analysis showed a correlation between *DMAPI* reduction and *MYCN* amplification (Table 1). These results suggested that *DMAPI* works as a tumour suppressor gene in NB and its expression levels strongly correlate with *MYCN* copy numbers.

### 3.2. *DMAPI* activated ATM and p53 with DNA damage

In our previous study, we observed that *Dmap1* knockdown in MEFs leads to the failure of DNA repair, resulting in accumulated DNA damage [11]. These results prompted us to study the role of *DMAPI* in DDR, including the ATM/p53 pathway. In response to DNA damage, ATM forms foci at double-stranded DNA break (DSB) sites and undergoes self-phosphorylation at serine 1981 to enhance its kinase activity. The activated ATM phosphorylates p53 at serine 15, which in turn induces p53-downstream effectors, leading to

Table 1  
Correlation between Dnmt1-associated protein 1 (*DMAPI*) expression and other prognostic factors of neuroblastoma.

Terms	High <i>DMAPI</i>	Low <i>DMAPI</i>	<i>p</i> -Value
Age (years)			
≤1.5	25	33	0.13
>1.5	31	23	
Tumour origin			
Adrenal	29	28	0.773
Others	26	28	
Stage			
1, 2, 4S	29	22	0.184
3, 4	27	34	
Shimada pathology			
Favourable	37	30	0.16
Unfavourable	12	18	
<i>MYCN</i> copy number			
Single	52	41	<0.01
Amplified	4	15	
<i>TrkA</i> expression			
High	32	28	0.507
Low	23	26	
DNA index			
Diploidy	22	27	0.186
Aneuploidy	28	20	

*MYCN*: Fisher's exact probability test,  $\chi^2 = 7.669496321$ ,  $p < 0.01$ .

the inhibition of cell cycle progression or apoptotic cell death [14]. For DNA damage induction, we chose doxorubicin (Doxo) at 0.5 µg/ml concentration to assess the effect on NB cells according to the results of the analysis of peak plasma concentrations of doxorubicin [15].

We expressed *DMAPI* in p53-wild type NB cells and found that ATM<sub>Ser1981</sub> phosphorylation increased for up to 6 h after Doxo treatment, and p53<sub>Ser15</sub> phosphorylation was up-regulated subsequently (Fig. 2A). We also confirmed *DMAPI*-related p53<sub>Ser15</sub> phosphorylation in human fibroblasts (Fig. 2B).

Next, SH-SY5Y cells, which express rather higher *DMAPI* than other NB cell lines (Suppl. Fig. S1D), were infected with sh*DMAPI*-expressing virus and treated with Doxo. Knockdown of *DMAPI* resulted in downregulation of ATM and p53 phosphorylation (Fig. 2C). We then evaluated the focus formation of ATM. It was significantly suppressed 1.0 h but not 1.5–2.5 h after Doxo treatment by *DMAPI* knockdown (Fig. 2D), suggesting that *DMAPI* is required for efficient focus formation of ATM in the early stage of DDR.

### 3.3. *DMAPI* activated p53 by ATM and induced transcription of p53-downstream genes

To examine whether p53 phosphorylation promoted by *DMAPI* is dependent on ATM activity, we used an

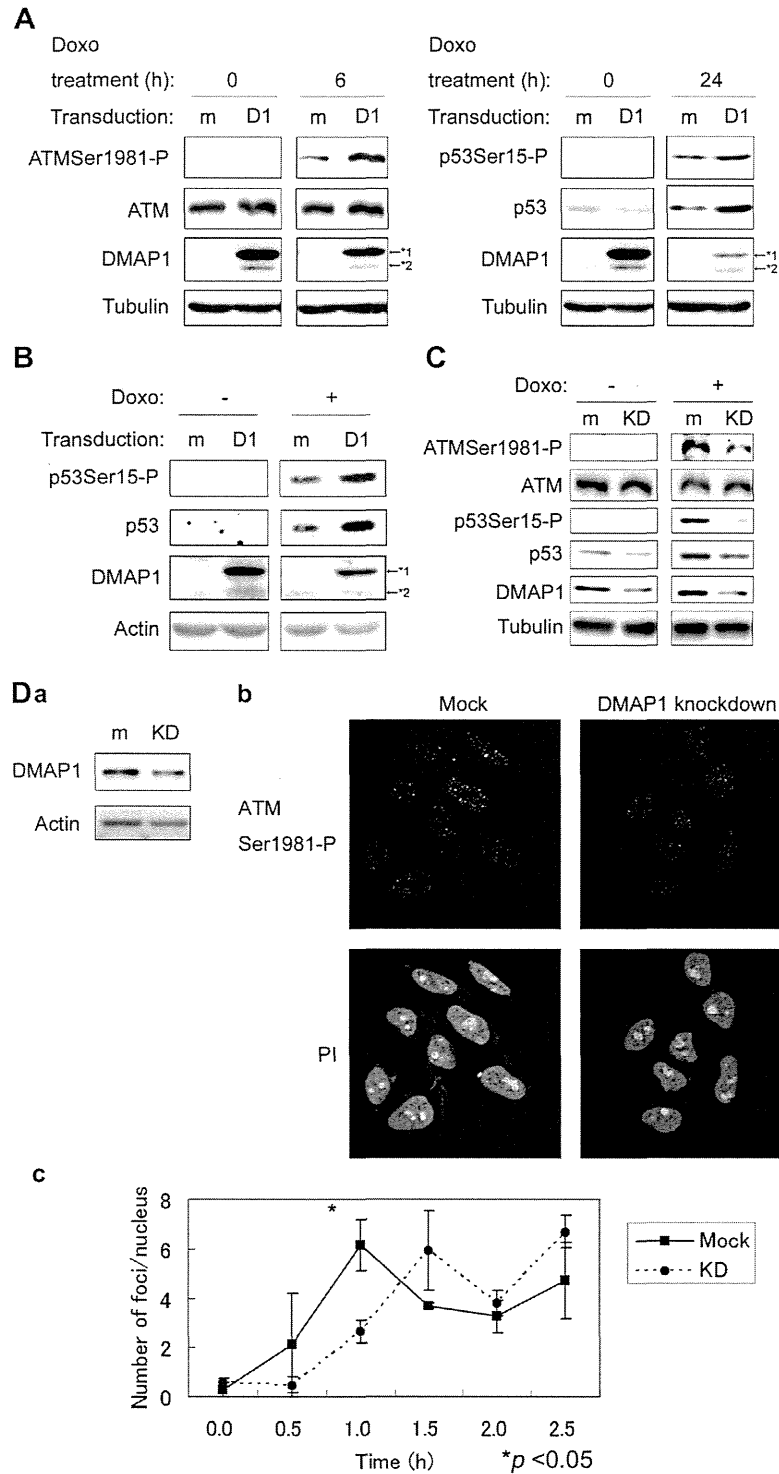


Fig. 2. Dnmt1-associated protein 1 (DMAP1) promoted focus formation of ataxia telangiectasia mutated (ATM) and activated ATM under doxorubicin (Doxo) treatment. (A) Phosphorylation status of ATMSer1981 and p53Ser15 in DMAP1 over-expressing cells. SK-N-SH cells were transduced with human influenza hemagglutinin (HA)-tagged DMAP1 and treated with Doxo for the indicated time period. The cells were subjected to sodium dodecyl sulphate–polyacrylamide gel electrophoresis (SDS–PAGE) and Western blot analysis. (B) Phosphorylation of p53Ser15 by DMAP1 in human fibroblasts (hfb). Hfb were transduced with HA-tagged DMAP1 and treated with Doxo for 24 h to confirm phosphorylation of p53 by Western blot analysis. (C) Phosphorylation status of ATMSer1981 in DMAP1 knocked-down cells. SH-SY5Y cells were infected with shDMAP1-expressing virus and treated with Doxo for 1 h. The cells were subjected to SDS–PAGE and Western blot analysis. (D) Focus formation of ATM in DMAP1 knocked-down cells. SH-SY5Y cells were infected with shDMAP1-expressing virus and treated with Doxo for the indicated time period, followed by SDS–PAGE, Western blot analysis (Da) and immunocytochemistry (ICC, Db). In ICC, cells were stained with anti-ATMSer1981-P and propidium iodide (PI). (Dc) Number of ATM foci was counted using the colony counting tool in Image Quant TL. Error bars represent S.D. obtained from triplicate samples. Data were analysed using the Welch test. Data are representative of three independent experiments. (A–D), m: mock, D1: DMAP1, KD: DMAP1 knockdown; \*1: HA-DMAP1, \*2: Endogenous DMAP1.

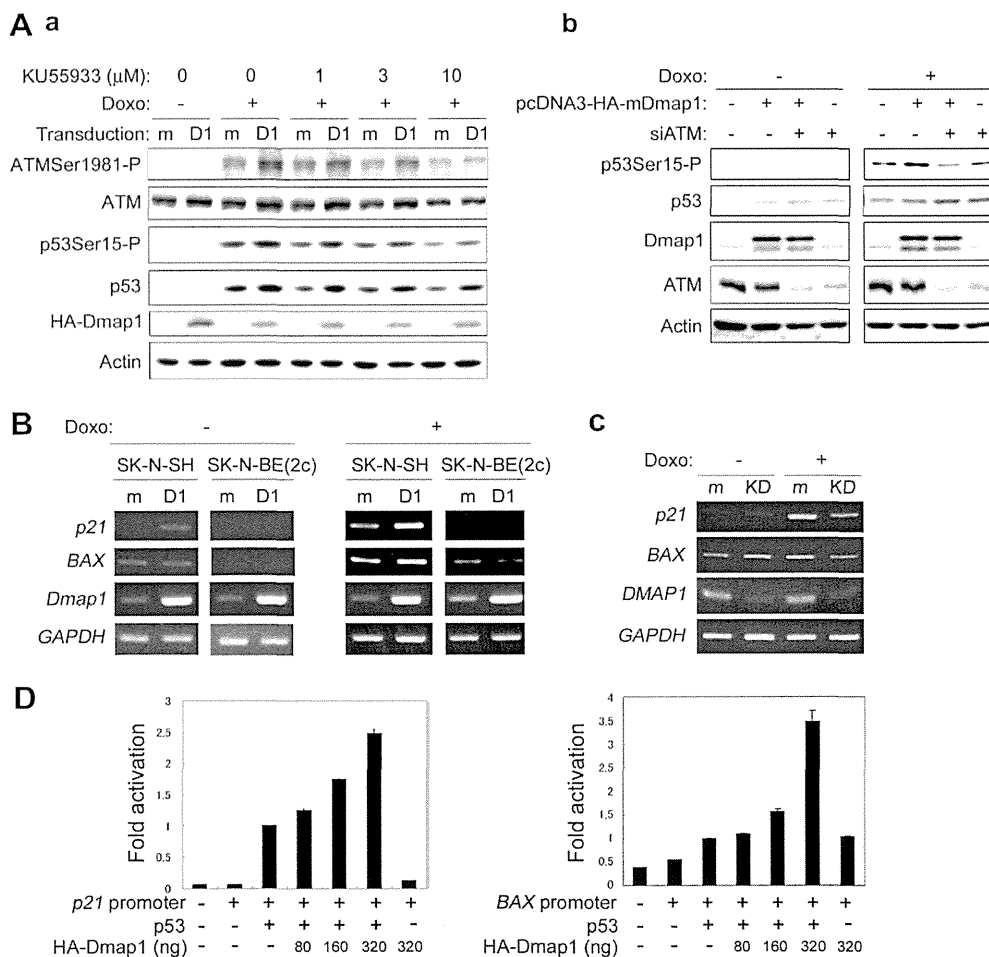


Fig. 3. Dnmt1-associated protein 1 (DMAP1) activated p53 via ataxia telangiectasia mutated (ATM). (A) Phosphorylation of p53Ser15 by Dmap1 through ATM activation. (Aa) SK-N-SH cells were infected with HA-tagged Dmap1-expressing virus and pre-treated with KU-55933. One hour after KU-55933 addition, cells were treated with doxorubicin (Doxo) for 12 h and subjected to sodium dodecyl sulphate–polyacrylamide gel electrophoresis (SDS–PAGE) and Western blot analysis. (Ab) SK-N-SH cells were transfected with *ATM* siRNA (sequence: 5'-AACATACTACTCAAAGACATT-3', Sigma–Aldrich, St. Louis, MO, USA) or control siRNA (ON-TARGETplus Non-targeting siRNA #1, Thermo Fisher Scientific, Lafayette, CO, USA). Transfection of siRNA was performed according to a previous report (16). Forty-eight hours after forward transfection, the cells were treated with 0.3 μg/ml Doxo for 1 h and subjected to Western blot. m: mock, D1: Dmap1. (B, C) Semi-quantitative Reverse Transcription Polymerase Chain Reaction (RT-PCR) of p53-target genes in *Dmap1* over-expressing cells (B) and in DMAP1 knocked-down SH-SY5Y cells (C). m: mock, D1: Dmap1, KD: DMAP1 knockdown. (D) Luciferase reporter assay analysis of *p21<sup>Cip1/Waf1</sup>* and *BAX* promoter activity in H1299 cells. Increasing amount of pcDNA3-HA-Dmap1, constant amount of pcDNA 3-p53, Renilla luciferase reporter plasmid (pRL-TK) and luciferase reporter plasmid with p53 responsive elements were transfected, and luciferase activity was studied. Data are representative of three independent experiments ( $n = 3$ ).

ATM-specific ATP-competitive inhibitor KU-55933. KU-55933 abrogated the Dmap1-induced phosphorylation of ATM and p53, indicating ATM dependency of Dmap1-related p53 phosphorylation (Fig. 3Aa). ATM knockdown further represented ATM-dependent p53Ser15 phosphorylation by DMAP1 (Fig. 3Ab). Downstream target genes of p53, such as *p21<sup>Cip1/Waf1</sup>* and *BAX*, were induced by Dmap1 in the presence or absence of Doxo in *p53*-wt SK-N-SH cells but were not induced in *p53*-mutated SK-N-BE(2c) cells (Fig. 3B). Knockdown of DMAP1 reduced p53 accumulation (Fig. 2C) and transcription of the downstream *p21<sup>Cip1/Waf1</sup>* and *BAX* in a Doxo-dependent manner (Fig. 3C). Transcription of *NOXA*, the pro-apoptotic

Bcl-2 family molecule, which was previously shown to be a critical molecule in p53-related damage-induced NB cell death [16], was also upregulated by DMAP1 (Suppl. Fig. S2A). DMAP1-promoted upregulation of *p21<sup>Cip1/Waf1</sup>* and *BAX* promoter activity, which was mediated by p53, was confirmed by a luciferase reporter assay of *p53*-null H1299 cells (Fig. 3D).

#### 3.4. DMAP1 acts as a tumour suppressor via p53 activation in NB cells

We examined the functional role of DMAP1 and its p53 dependency in NB cells. DMAP1 enhanced cell cycle arrest and apoptosis induced by Doxo in a

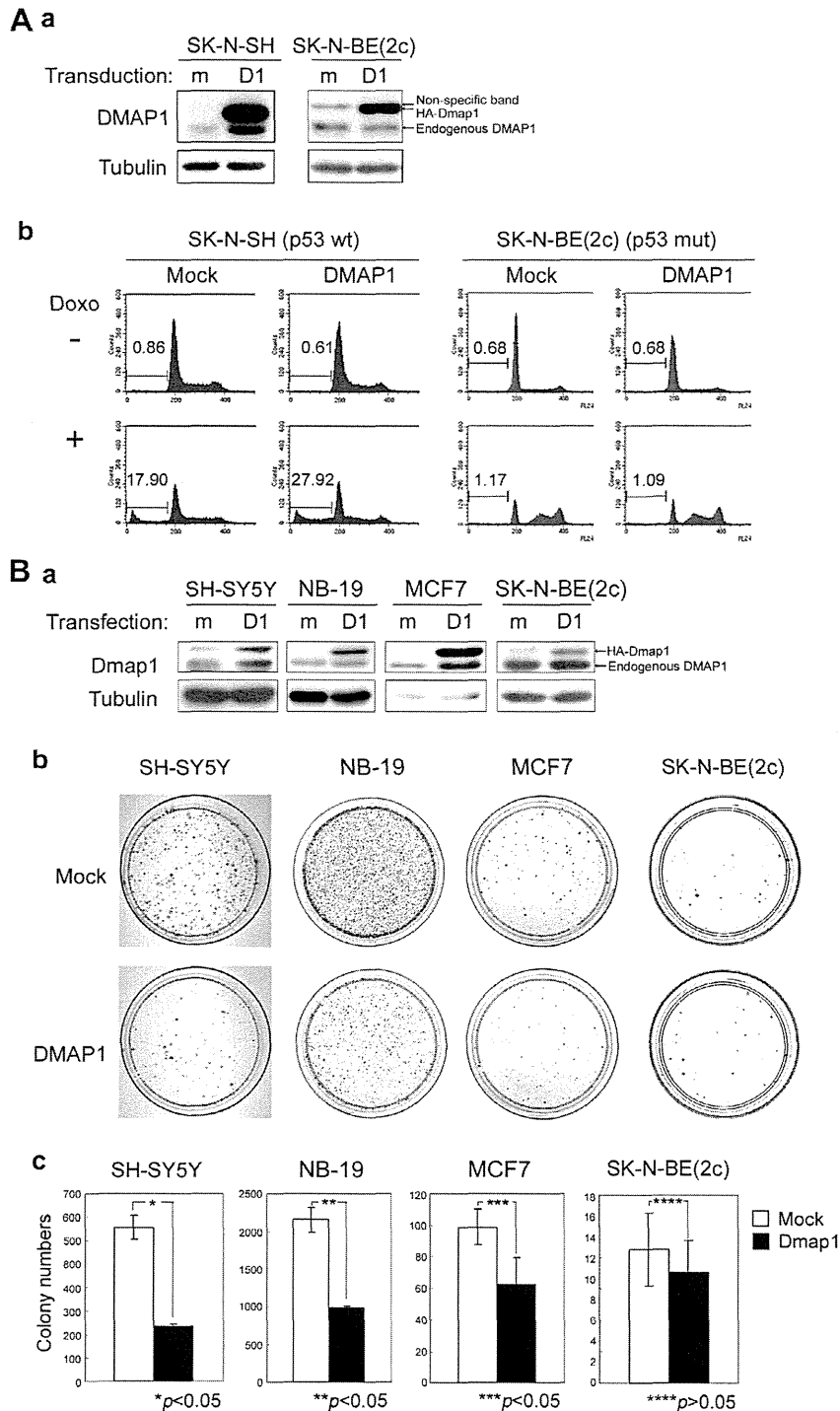


Fig. 4. Dnmt1-associated protein 1 (DMAP1) acts as a tumour suppressor via p53 activation in NB cells. (A) Dmap1-transduced NB cells were treated with doxorubicin (Doxo) and subjected to Western blot (Aa) and cell cycle analysis by flow cytometry (Ab). Numbers in histogram indicate % of subG0/G1 population. (B) Colony formation assay in Dmap1 over-expressing cells. Cells were transfected with pcDNA3-heteroduplex analysis (HA)-Dmap1 and subjected to Western blot (Ba) and selected with 400 µg/ml G418 for SH-SY5Y cells, 500 µg/ml G418 for NB-19 cells, 800 µg/ml G418 for MCF7 cells and 800 µg/ml G418 for SK-N-BE(2c) cells, for 2 weeks. (Bb) Colonies were stained with May-Grünwald's Eosin Methylene Blue Solution (Wako, Osaka, Japan) and Giemsa's solution (Merk Japan, Tokyo, Japan). (Bc) Number of colonies was counted using the colony counting tool in Image Quant TL. Error bars represent S.D. (A–B), m: mock, D1: Dmap1.

p53-dependent manner (Fig. 4A and Suppl. Fig. S2B). SH-SY5Y cells, NB-19 cells and breast cancer-derived MCF7 cells harbouring wild-type p53 were transfected with pcDNA3-HA-Dmap1 and selected with G418 for

two weeks. As shown in Fig. 4B, Dmap1 significantly suppressed colony formation in these cells. These results suggested that DMAP1 acts as a tumour suppressor via p53 activation in NB cells.



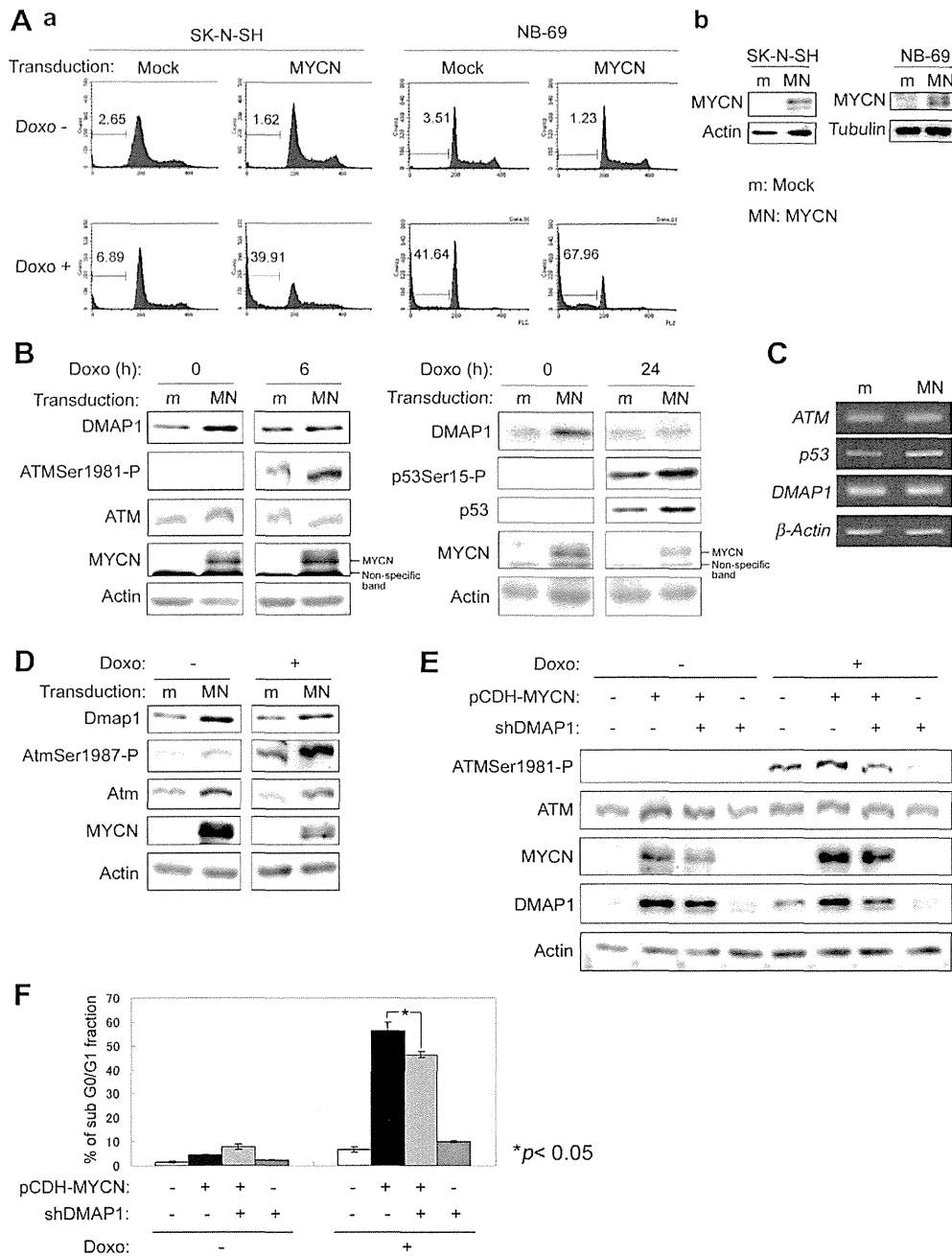


Fig. 5. MYCN promoted doxorubicin (Doxo)-induced apoptosis and ataxia telangiectasia mutated (ATM)/p53 activation. Cells were transduced with pCDH-MYCN and subjected to analysis as follows. (Aa) Cell cycle analysis [(Ab) protein expression was confirmed by Western blotting in left panel], (B) Western blot analysis and (C) semi-quantitative RT-PCR of MYCN over-expressing and Doxo-treated NB cells. Numbers in histogram indicate % of sub G0/G1 population. (D) Activation of Atm/p53 pathway by MYCN in NIH3T3 cells. Cells were collected 12 h after Doxo treatment and subjected to Western blot analysis. (E, F) MYCN over-expression and/or Dnmt1-associated protein 1 (DMAP1) knockdown were performed as indicated in SK-N-SH cells. Cells were collected for Western blot analysis of ATM Ser1981-P (E) and sub G0/G1 analysis (F) 6 h after Doxo treatment. (A–D) m: mock, MN: MYCN.

### 3.5. DMAP1 was implicated in MYCN-induced ATM activation

Given that MYCN amplification correlated with a low level of DMAP1 and that MYCN regulates the ATM/p53 pathway [17], we studied the DMAP1/ATM/p53 pathway in MYCN-transduced cells. As

reported [18], exogenous MYCN promoted apoptosis in MYCN single-copy and p53 wild type SK-N-SH cells and NB-69 cells (Fig. 5A) and activation of ATM/p53 under Doxo treatment in SK-N-SH cells (Fig. 5B left: 6 h after, right: 24 h after). Interestingly, the protein amount of DMAP1 was upregulated by MYCN although DMAP1 mRNA was not increased (Fig. 5B, C).

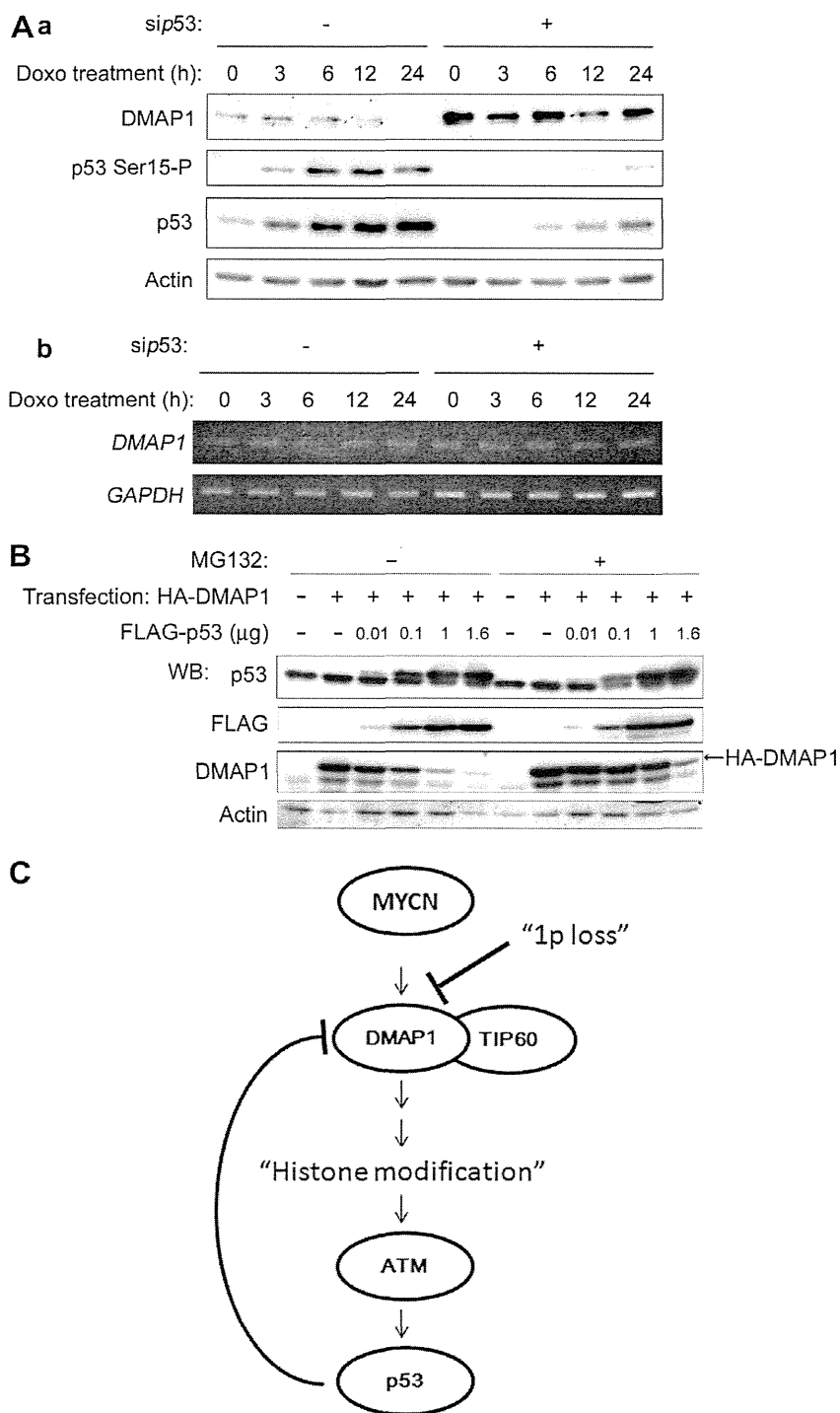


Fig. 6. Dnmt1-associated protein 1 (DMAP1) degradation by p53. (A) DMAP1 expression in p53 knocked-down cells. SK-N-SH cells harbouring wt-p53 were transfected with *p53* siRNA (ON-TARGETplus Duplex J-003329-14-0005, Human Tp53; Thermo Fisher Scientific, Lafayette, CO, USA) or control siRNA (Silencer\_Negative Control #1 siRNA; Ambion Inc., Austin, TX, USA). Transfection of siRNA was performed according to a previous report (16). Forty-eight hours after forward transfection, the cells were treated with 0.3  $\mu$ g/ml doxorubicin (Doxo) for the indicated time periods and subjected to Western blotting (Aa)/semi-quantitative RT-PCR (Ab). (B) Western blot analysis of Dmap1 degradation by p53 in combination with MG132 treatment. 293T cells were transfected with a constant amount of pcDNA3-heteroduplex analysis (HA)-tagged Dmap1 and increasing amounts of pcDNA3-FLAG-tagged p53 and then treated with 2  $\mu$ M MG132 for 24 h. (C) MYCN/DMAP1/ataxia telangiectasia mutated (ATM)/p53 pathway regulates neuroblastoma cell death.

These phenomena were confirmed in *MYCN*-single copy, p53 wild-type NIH3T3 fibroblasts (Fig. 5D).

Further, DMAP1 knockdown reduced the phosphorylation of ATM (Fig. 5E) and Doxo-induced apoptosis

(Fig. 5F), which were up-regulated by MYCN, indicating that DMAP1 was implicated in MYCN-induced ATM/p53 activation and apoptosis.

### 3.6. Negative feedback regulation of DMAP1 by p53

In MYCN-related ATM/p53 pathway activation, we found that DMAP1 protein was reduced, accompanied with p53 activation (Fig. 5B) and this DMAP1 reduction was also observed in DMAP1-transduced cells after p53 activation by Doxo (Figs. 2A, B and 3A). To examine whether p53 reduces DMAP1, we knocked down p53 in NB cells (Fig. 6A). DMAP1 protein was clearly increased by p53 knockdown, but the mRNA level of DMAP1 was not affected. Proteasome inhibitor, MG132 treatment effectively inhibited DMAP1 degradation by p53 expression (Fig. 6B), suggesting that p53 promotes DMAP1 degradation in an ubiquitin-proteasome system-dependent manner.

## 4. Discussion

The proto-oncogenes *MYC* and *MYCN* have a pivotal function in growth control, differentiation and apoptosis and are among the most frequently affected genes in human malignant tumours; they are overexpressed in a large percentage of human tumours [19,20]. Transformation by Myc proteins requires concomitant inhibition of apoptosis by inactivation of apoptosis-inducing pathway genes [21]. One of the *MYC* oncogene product-related apoptotic pathways is involved in DDR [18]. Recent studies have clarified the relevant pathways regulating MYC-induced DDR, leading to the identification of ATM, TIP60 and WIP1 as mediators of this response [22]. Once ATM was activated by DNA damage, both p53 and proteins that interact with p53, MDM2 and Chk2 were phosphorylated by ATM, which in turn transactivated the p53-downstream effectors, leading to the inhibition of cell cycle progression or apoptotic cell death [23].

Regarding MYC/MYCN-related ATM regulation, this over-expression causes DNA damage *in vivo* and the ATM-dependent response to this damage is critical for p53 activation, apoptosis and the suppression of tumour development [22,24,25]. These findings suggested that MYC/MYCN expression induces ATM/p53 pathway activation by the related cellular stresses and subsequent inactivation of ATM will produce advantages for the tumorigenesis of MYC/MYCN-deregulated tumours. However, the occurrence of NB in ataxia-telangiectasia patients and ATM mutation in NB cells have not been reported to our knowledge, and mutations of p53 have been reported in <2% of NB [26,27], suggesting that functional inactivation of the pathway by other molecules seems to occur in NB tumours.

In the present study, we found that MYCN expression in *MYCN* single-copy cells increased DMAP1 and Doxo-induced apoptotic cell death (Fig. 5). DMAP1 induced ATMSer1981 phosphorylation and its focus formation in the presence of Doxo (Figs. 2 and 3A). By DMAP1 expression, p53Ser15 phosphorylation was induced in an ATM-dependent manner. In NB tumour samples, low expression of DMAP1 was related to poor prognosis, unfavourable histology, *MYCN* amplification and 1p LOH (Fig. 1, Table 1, Suppl. Fig. S1), suggesting that DMAP1 downregulation is required for NB tumourigenesis, especially under MYCN-induced cellular stress. Intriguingly, we observed negative feedback for degrading DMAP1, suggesting another DMAP1 downregulation mechanism in NB tumourigenesis (Fig. 6).

Recently, Penicud and Behrens reported that DMAP1 enhances Histone Acetyl Transferase (HAT) activity of TIP60 and promotes ATM auto-phosphorylation [12]. Depleting DMAP1 reduced ATM phosphorylation a few minutes after irradiation, but at later time points, it had no effect on ATM activation, as we previously reported [11]. Consistent with these observations, we found that DMAP1 knockdown delayed ATM focus formation and that the delay of ATM activation attenuated p53 phosphorylation and stabilisation. (Fig. 2C, D). These results indicate that DMAP1 regulates the efficient recruitment of ATM to the site of DNA breaks and this regulation is required for subsequent Doxo-induced p53-dependent cell death in NBs.

Taken together, we found that DMAP1 is a novel molecule of 1p tumour suppressors and has a role in ATM/p53 activation induced by MYCN-related cellular stresses (Fig. 6C). DMAP1 might be a new molecular target of MYCN-amplified NB treatment.

### Conflict of interest statement

None declared.

### Acknowledgements

We would like to thank Ms. Kumiko Sakurai and Dr. Masamitsu Negishi for technical help, and Daniel Mrozek, Medical English Service, for editorial assistance. *Grant Support:* This work was supported in part by a grant-in-aid from the National Cancer Center Research and Development Fund (4), a grant-in-aid from the Ministry of Health, Labor, and Welfare for Third Term Comprehensive Control Research for Cancer, and a Grant-in-Aid for Scientific Research (B) (24390269).

### Appendix A. Supplementary data

Supplementary data associated with this article can be found, in the online version, at <http://dx.doi.org/10.1016/j.ejca.2014.01.023>.

## References

- [1] Brodeur GM. Neuroblastoma: biological insights into a clinical enigma. *Nat Rev Cancer* 2003;3:203–16.
- [2] Praml C, Finke LH, Herfarth C, Schlag P, Schwab M, Amler L. Deletion mapping defines different regions in 1p34.2-pter that may harbor genetic information related to human colorectal cancer. *Oncogene* 1995;11:1357–62.
- [3] Nagai H, Negrini M, Carter SL, et al. Detection and cloning of a common region of loss of heterozygosity at chromosome 1p in breast cancer. *Cancer Res* 1995;55:1752–7.
- [4] Smith JS, Perry A, Borell TJ, et al. Alterations of chromosome arms 1p and 19q as predictors of survival in oligodendrogliomas, astrocytomas, and mixed oligoastrocytomas. *J Clin Oncol* 2000;18:636–45.
- [5] Yang J, Du X, Lazar AJ, et al. Genetic aberrations of gastrointestinal stromal tumors. *Cancer* 2008;113:1532–43.
- [6] Maris JM, Weiss MJ, Guo C, et al. Loss of heterozygosity at 1p36 independently predicts for disease progression but not decreased overall survival probability in neuroblastoma patients: a Children's Cancer Group study. *J Clin Oncol* 2000;18:1888–99.
- [7] Martinsson T, Sjöberg RM, Hedborg F, Kogner P. Deletion of chromosome 1p loci and microsatellite instability in neuroblastomas analyzed with short-tandem repeat polymorphisms. *Cancer Res* 1995;55:5681–6.
- [8] White PS, Thompson PM, Gotoh T, et al. Definition and characterization of a region of 1p36.3 consistently deleted in neuroblastoma. *Oncogene* 2005;24:2684–94.
- [9] Hogarty MD, Winter CL, Liu X, et al. No evidence for the presence of an imprinted neuroblastoma suppressor gene within chromosome sub-band 1p36.3. *Cancer Res* 2002;62:6481–4.
- [10] Rountree MR, Bachman KE, Baylin SB. DNMT1 binds HDAC2 and a new co-repressor, DMAP1, to form a complex at replication foci. *Nat Genet* 2000;25:269–77.
- [11] Negishi M, Chiba T, Saraya A, Miyagi S, Iwama A. Dmap1 plays an essential role in the maintenance of genome integrity through the DNA repair process. *Genes Cells* 2009;14:1347–57.
- [12] Penicud K, Behrens A. DMAP1 is an essential regulator of ATM activity and function. *Oncogene* 2014;33:525–31.
- [13] Takenobu H, Shimozato O, Nakamura T, et al. CD133 suppresses neuroblastoma cell differentiation via signal pathway modification. *Oncogene* 2011;30:97–105.
- [14] Lavin MF. Ataxia-telangiectasia: from a rare disorder to a paradigm for cell signalling and cancer. *Nat Rev Mol Cell Biol* 2008;9:759–69.
- [15] James HD. Topoisomerase II inhibitors: anthracyclines. In: Chabner BA, Longo DL, editors. *Cancer chemotherapy and biotherapy: principles and practice*. Philadelphia: Lippincott Williams & Wilkins, a Wolters Kluwer Business; 2011. p. 356–91.
- [16] Shi Y, Takenobu H, Kurata K, et al. HDM2 impairs Noxa transcription and affects apoptotic cell death in a p53/p73-dependent manner in neuroblastoma. *Eur J Cancer* 2010;46:2324–34.
- [17] Hu H, Du L, Nagabayashi G, Seeger RC, Gatti RA. ATM is down-regulated by N-Myc-regulated microRNA-421. *Proc Natl Acad Sci U S A* 2010;107:1506–11.
- [18] Fulda S, Lutz W, Schwab M, Debatin KM. MycN sensitizes neuroblastoma cells for drug-induced apoptosis. *Oncogene* 1999;18:1479–86.
- [19] Evan GI, Littlewood TD. The role of c-myc in cell growth. *Curr Opin Genet Dev* 1993;3:44–9.
- [20] Schwab M, Alitalo K, Klempnauer KH, et al. Amplified DNA with limited homology to myc cellular oncogene is shared by human neuroblastoma cell lines and a neuroblastoma tumour. *Nature* 1983;305:245–8.
- [21] Gustafson WC, Weiss WA. Myc proteins as therapeutic targets. *Oncogene* 2010;29:1249–59.
- [22] Campaner S, Amati B. Two sides of the Myc-induced DNA damage response: from tumor suppression to tumor maintenance. *Cell Div* 2012;7:6.
- [23] Derheimer FA, Kastan MB. Multiple roles of ATM in monitoring and maintaining DNA integrity. *FEBS Lett* 2010;584:3675–81.
- [24] Petroni M, Veschi V, Prodosmo A, et al. MYCN sensitizes human neuroblastoma to apoptosis by HIPK2 activation through a DNA damage response. *Mol Cancer Res* 2011;9:67–77.
- [25] Swift M, Reitnauer PJ, Morrell D, Chase CL. Breast and other cancers in families with ataxia-telangiectasia. *N Engl J Med* 1987;316:1289–94.
- [26] Vogan K, Bernstein M, Leclerc JM, Brisson L, Brossard J, Brodeur GM, et al. Absence of p53 gene mutations in primary neuroblastomas. *Cancer Res* 1993;53:5269–73.
- [27] Tweddle DA, Malcolm AJ, Bown N, Pearson AD, Lunec J. Evidence for the development of p53 mutations after cytotoxic therapy in a neuroblastoma cell line. *Cancer Res* 2001;61:8–13. <http://cancerres.aacrjournals.org/content/61/1/8.long>.